Ornelas-Hernández *et al.*
Nanoscale Research Letters (2022) 17:56
https://doi.org/10.1186/s11671-022-03691-7

Nanoscale Research Letters

NANO REVIEW

Open Access

A Brief Review of Carbon Dots–Silica Nanoparticles Synthesis and their Potential Use as Biosensing and Theragnostic Applications

Luis Fernando Ornelas-Hernández[1], Angeles Garduno-Robles[1] and Abraham Zepeda-Moreno[1,2,3*]

Abstract

Carbon dots (CDs) are carbon nanoparticles with sizes below 10 nm and have attracted attention due to their relatively low toxicity, great biocompatibility, water solubility, facile synthesis, and exceptional photoluminescence properties. Accordingly, CDs have been widely exploited in different sensing and biomedical applications, for example, metal sensing, catalysis, biosensing, bioimaging, drug and gene delivery, and theragnostic applications. Similarly, the well-known properties of silica, such as facile surface functionalization, good biocompatibility, high surface area, and tunable pore volume, have allowed the loading of diverse inorganic and organic moieties and nanoparticles, creating complex hybrid nanostructures that exploit distinct properties (optical, magnetic, metallic, mesoporous, etc.) for sensing, biosensing, bioimaging, diagnosis, and gene and drug delivery. In this context, CDs have been successfully grafted into diverse silica nanostructures through various synthesis methods (e.g., solgel chemistry, inverse microemulsion, surfactant templating, and molecular imprinting technology (MIT)), imparting hybrid nanostructures with multimodal properties for distinct objectives. This review discusses the recently employed synthesis methods for CDs and silica nanoparticles and their typical applications. Then, we focus on combined synthesis techniques of CD–silica nanostructures and their promising biosensing operations. Finally, we overview the most recent potential applications of these materials as innovative smart hybrid nanocarriers and theragnostic agents for the nanomedical field.

Keywords: Carbon dots, Nanoparticles, Carbon dots–silica nanoparticles

Introduction

In recent years, the innovative field of nanotechnology has led to novel applications in diverse scientific disciplines due to the fascinating physical chemistry properties of nanosized materials (1–100 nm) and their interactions with other systems that exist at the molecular level (e.g., atoms and molecules) [1]. The development of devices at the nanoscale has revealed improved functions of multiple materials compared to their bulk version. Nanomaterials can be produced by using different physical (top-down) and chemical (bottom-up) synthesis methods, which can occur in the gas phase, liquid phase, and solid phase. Some examples of physical synthesis techniques include pulsed laser ablation in liquid (PLAL) [2], laser ablation, laser pyrolysis, microwave irradiation [3], chemical vapor deposition (CVD), physical vapor deposition (PVD), etching, electric explosion, high-energy ball milling, and electric arc deposition. Chemical synthesis techniques include the following: coprecipitation, hydrothermal synthesis, solvothermal synthesis, microemulsion, solgel, chemical reduction, spray pyrolysis, electrochemical synthesis, green synthesis, and biological synthesis. Selection of an appropriate nanomaterial synthesis method depends on various factors, such as available infrastructure, costs, performance, large scale, and ecofriendliness [4]. Additionally, each synthesis method allows obtaining specific nanomaterial

*Correspondence: abraham.zepeda@mxaib.com

[1] Onkogenetik/Mexicana de Investigación Y Biotectogía SA. de C.V., Av. Miguel Hidalgo y Costilla 1966, Guadalajara, Jalisco, México
Full list of author information is available at the end of the article

Springer Open

© The Author(s) 2022. **Open Access** This article is licensed under a Creative Commons Attribution 4.0 International License, which permits use, sharing, adaptation, distribution and reproduction in any medium or format, as long as you give appropriate credit to the original author(s) and the source, provide a link to the Creative Commons licence, and indicate if changes were made. The images or other third party material in this article are included in the article's Creative Commons licence, unless indicated otherwise in a credit line to the material. If material is not included in the article's Creative Commons licence and your intended use is not permitted by statutory regulation or exceeds the permitted use, you will need to obtain permission directly from the copyright holder. To view a copy of this licence, visit http://creativecommons.org/licenses/by/4.0/.

characteristics and physical chemistry properties. These remarkable properties (surface area, optical, mechanical, magnetic, quantum effect, electrical conductivity, high thermal resistance) can be obtained by controlling the particle size and shape [5, 6]. Therefore, nanomaterials are excellent candidates to resolve, improve, or generate new promising applications in electronics, energy storage [7], biomedicine, biotechnology, pharmaceutical sensing, photocatalysis, and water remediation, among others [8, 9]. Regarding nanomedicine and biosensing, the most exploited nanomaterials properties are the optical, magnetic, and thermal properties and large surface area. For example, metallic nanoparticles known as plasmonic nanoparticles (containing gold, silver, copper, etc.) exhibit strong absorption in the visible region and a specific localized surface plasmon resonance (LSPR) [10]. This property of absorption and light scattering can be used for colorimetric sensing of biological species (e.g., DNA, aptamers, antibodies, proteins, carbohydrates, and lipids) [11] as well as for photothermal therapy (PTT), drug delivery and in vivo and in vitro imaging. In a similar manner, superparamagnetic nanoparticles (SMPs, e.g., Fe oxides and gadolinium) have been applied to the same applications mentioned above and as magnetic resonance imaging (MRI) contrast agents for the magnetic separation of biological moieties and induction of magnetic hyperthermia [12]. Other nanomaterials that present extraordinary properties for nanomedical and sensing applications are inorganic fluorescent nanoparticles [13]. A typical example of these nanomaterials is quantum dots (QDs), which are nanocrystals of semiconductor oxides and chalcogenides (e.g., ZnO, CdS, and CdSe). The fluorescence of QDs is related to the quantum confinement effect and the band gap, which produces a shift in the emission wavelength with respect to the particle size. In addition to QDs, other optical nanomaterials that have been developed for sensing and nanomedical applications include upconversion nanoparticles and, recently, CDs and graphene QDs. CDs are spherical nanostructures obtained by different synthetic methods using organic natural materials as synthetic precursors. The optical properties (high quantum yield, resistance to photobleaching, narrow emission, etc.) of all mentioned photoluminescent nanomaterials, including CDs, are notably superior to those of traditional organic dyes, which makes them suitable options for the design of highly sensitive biosensors. In contrast to QDs, CDs are obtained by straightforward methods that notably diminish the time and resources required for their production. Additionally, the outstanding optical properties of CDs significantly reduce the time required for obtaining reproducible results in sensing and optical assays, without the requirement of qualified personnel; moreover, these properties help to avoid the use of costly and complex equipment. On the other hand, owing to the biocompatibility, high surface area, tunable pore diameter, length, and spatial structure of silica-based nanomaterials, including nanoparticles and mesoporous structures, these materials are fundamental for the development of new multifunctional sensing and nanomedical devices.

The unique properties of the above-mentioned nanomaterials have motivated researchers to engineer complex nanostructures with different characteristics for multiple objectives. For instance, the creation of engineered hybrid nanostructures has been reported, where at least one of the elements is stimuli responsive, while the other has drug cargo properties. Such systems have shown improvements in drug delivery systems (DDSs) since the stimuli-responsive material allows drug release control both spatially and temporally. Some authors have engineered dynamic nanosystems that make use of "nanovalves" through self-assembly and supramolecular interactions. These tools act as open–close gates or "gatekeepers" that are activated by diverse stimuli (e.g., pH, redox potential, thermal, magnetic, and enzymatic stimuli) [14]. These outstanding mechanisms allow the production of nonburst, true controlled release systems.

CD–silica hybrid nanomaterials are ideal for the above-mentioned features and applications. First, CDs exhibit both outstanding optical properties and excellent biocompatibility. Moreover, silica nanomaterials are ideal nanocontainers for numerous species including small organic molecules, macromolecules, and nanoparticles. From this aspect, in this review, we will first discuss the synthesis and applications of CDs and silica nanoparticles. These two nanomaterials exhibit different properties. On the one hand, CDs have outstanding fluorescent properties; on the other hand, silica and its derivatives have the advantages of cargo capacity, large surface area, ordered pore structure, etc. Then, we summarize the combination of CDs/silica into one nanostructure (nanocomposite), the synthesis techniques and how some researchers have used this second-generation nanostructure for recent applications in biosensing and nanomedicine.

Carbon Dots

Since the discovery of CDs through the electrophoretic purification of single-walled carbon nanotubes, which arose as by-products of the arc-discharge of soot [15], CDs have attracted attention due to their fascinating unusual physical and chemical features, such as emissive optical properties, high quantum yield, resistance to photobleaching, superior photostability, excellent water solubility, good biocompatibility, chemical inertness and low toxicity. Currently, it is known that the

difference between CDs and their analogs, graphene QDs, is that CDs are quasispherical nanoparticles with diameters < 10 nm, composed of a sp^2 carbogenic core surrounded by an amorphous sp^3 carbon matrix, while graphene QDs possess higher crystallinity owing to the presence of mono- or multilayered graphite cores. Some experimental approaches have been proposed to elucidate the intrinsic photoluminescence generation mechanism of CDs, supported by theoretical computational modeling such as density functional theory (DFT) and time-dependent DFT calculations. Multiple authors suggest that unlike that of metallic QDs, the emission color of CDs does not depend on the nanoparticle size; instead, the emission is associated with different factors including the nature of the starting synthetic precursors, energy states, emissive traps, surface defects, and radiative recombination of excitons [16, 17]. Other authors claim that the emission is due to the formation of molecular fluorophores as side products during synthesis [18]; however, the nature of the photoluminescence is not yet clear [17, 19, 20]. Regarding chemical and biological aspects, the high content of carbon atoms and the heteroatoms in CDs confer them chemical characteristics such as high water solubility and, at the same time, grant them excellent biocompatibility.

Carbon Dot Synthesis and Applications

The first characterizations of CD fluorescence showed that photoluminescence is an *excitation-independent emission* since CDs generally emit blue color, and depending on their superficial states, they might also emit another wavelength with lower intensity. Nevertheless, these emissions require different wavelength excitation sources. Therefore, to produce excitation-independent emission CDs that emit from a single wavelength excitation source, different strategies, such as engineering of surface chemistry and functional group heteroatom doping [21], have been applied. These approaches have been applied in conjunction with diverse top-down (e.g., microwave irradiation and laser ablation) and bottom-up (e.g., hydrothermal synthesis, carbonization, pyrolysis, and electrochemistry) synthesis methods [22–32]. Notably, CDs can be generated using organic natural sources and synthetic precursors that are selected to provide tunable fluorescence properties and functionalization for specific targeting ligands [33–38]. CDs have shown outstanding photophysical, photochemical, electroluminescent, and electrochemical properties. Some of these properties such as phosphorescence, photoluminescence, strong absorption, quantum confinement effects, high electrical conductivity, surface defects, and charge transfer effects have been exploited in diverse areas including biomedicine, forensic science, and electronic and storage and conversion of energy. In the last two areas mentioned, CDs have shown interesting promising applications in the fabrication of supercapacitors, rechargeable and lithium-ion batteries, light-emitting diodes (LEDs), organic light-emitting devices, luminophores, coreactants, solar cells, cathode and anodes, and in nanophotocatalysis, nano-organocatalysis, information encryption, and sensors [39, 40] (Table 1).

Carbon Dots in Biomedical Applications

Due to the fascinating properties of CDs such as low cytotoxicity, high water solubility, biocompatibility and the photophysical and photochemistry properties mentioned in the previous section, these materials have been exploited in different biomedical applications. Examples include biosensors [41, 42], drug administration, allowing the controlled release of drugs [43], gene delivery, bioimaging, photoacoustic imaging, and photothermal and photodynamic therapy [44, 45] (Table 2) [46–53]. Kong et al. [54] produced functionalized CDs by using hydrothermal methods with phenylenediamine and ethylenediamine as precursors. Surface modification of CDs was used to promote electron transport. This investigation showed that the CDs were successfully employed as reactive oxygen species (ROS) scavengers in murine models, mimicking peroxidase (POD), catalase (CAT), and superoxide dismutase (SOD). These achievements demonstrated that CDs can be used in nanocatalytic medicine as excellent therapeutic agents for inflammatory liver diseases [50]. Yang et al. [55] developed CDs by a hydrothermal technique for use in gene delivery and cancer cell detection. The authors strategically incorporated polyethyleneimine (PEI) and folic acid (FA) into the CDs to facilitate biological interactions. The positively charged PEI molecules served as DNA-binding molecules, and folate

Table 1 Examples of common usable applications of CDs

Sensing applications	References
Be2 + ions detection	[21]
Selective detection of tartrazine in food samples	[34]
2,4,6-Trinitrophenol detection	[39]
Silver ions detection	[40]
Energy and environmental applications	
Photocatalysis degradation of naphthol blue black	[38]
Nanocatalysts oxidation of cyclohexane	[50]
Hypochlorite (ClO −) detection	[51]
Electroluminescent LEDs production	[59]
Photoluminescent LEDs production	[60]
Printing text and 3D printing	[41]
Solar cell devices	[17]

Table 2 Biomedical applications

Starting precursor	Synthesis method	Use	Application	References
Sargassum fluitans	Hydrothermal	DNA detection	Biosensors	[72]
Urea/citric acid	Solvothermal	RNA detection		[73]
o-Phenylenediamine, 2-aminoterephthalic acid	Solvothermal	microRNA-21 detection		[56]
Citric acid, basic fuchsin	Hydrothermal	Intracellular pH sensing		[74]
Citric acid, ethylenediamine	Hydrothermal	Spectrofluorometric detection of cancer cells		[75]
Diammonium hydrogen citrate	Pyrolysis	*Escherichia coli* and iron(III) detection		[36]
Poly(ethylene glycol) (PEG800), cyanine dye	Solvothermal	Near-infrared fluorescence imaging and photothermal cancer therapy	In vivo and in vitro imaging	[76]
Citric acid, polyethyleneimine (PEI)	Hydrothermal	Lysosome labeling and imaging		[77]
Polyethyleneimine (PEI)	Hydrothermal	Gene/drug delivery/imaging		[78]
Citric acid, thiourea, 3-aminophenylboronic acid	Hydrothermal	Glucosamine and liver cancer cell imaging		[79]
Carrot	Hydrothermal	Ratiometric two-photon fluorescence turn-on sensing of sulfide anion in biological fluids		[37]
Polyethyleneimine (PEI), folic acid (FA)	Hydrothermal	Gene therapy	Drug and gene delivery	[55]

served as a receptor. The nanomaterial demonstrated the ability to detect 293 T and HeLa cells and presented plasmid transfection activity [56, 57]. Recently, new trends in the applications of CDs have emerged. Naik et al. [58] produced pink fluorescent CDs for photomedicine. The authors showed that these pink fluorescent CDs can be applied for cancer cell bioimaging, antibacterial activity, and ROS scavenging. Another new topic regarding biomedical application of CDs is related to covering all spectral regions, particularly the near-infrared region [59–62]. Nevertheless, despite all these promising applications of CDs, to date, it is necessary to establish an effective large-scale production synthesis method, standardize the composition and structure of CDs, and achieve a better yield [63–69]. In addition, a better comprehension of the nature of the photoluminescence properties is needed [59, 70]. Li et al. [71] reported and interestingly achieved the large-scale production of CDs by an aldol condensation reaction at room temperature and ambient pressure. As a result, the authors produced a 1.083 kg CD batch.

Silica Nanoparticle Synthesis and Applications

The obtention of silica nanoparticles involves the well-known solgel processing method, in which hydrolysis and condensation reactions (see Eq. 1 and Eq. 2) of common metal alkoxides (e.g., tetraethyl orthosilicate (TEOS) and tetramethyl orthosilicate (TMOS)) take place, either under acidic or under basic conditions. Additionally, other precursors such as transition metals (Ti and Zr), alkoxides, aluminates, and borates can be used. By controlling a series of factors, such as reaction time, gelation, aging, and drying, this synthetic route can produce colloidal silica, oxide films, gels (aerogels and xerogels), or ceramic materials [80].

Hydrolysis:

$$\mathrm{Si(OR)_4 + H_2O \rightarrow HO - Si(OR)_3 + ROH} \quad (1)$$

Condensation:

$$\mathrm{(OR)_3Si - OH + HO - Si(OR)_3 \rightarrow (OR)_3Si - O - Si(OR)_3 + H_2O} \quad (2)$$

One of the most important methods for silica nanoparticle production was reported by Stöber et al. [81]. The authors were able to produce monodispersed silica spheres with diameters of a few microns through the hydrolysis of alkyl silicates in a mixed solution of alcohol and ammonia. Over the years, this synthesis method has been modified or adapted for different purposes [82]. For example, compared to the traditional Stöber method, the use of the Stöber method in combination with an inverse microemulsion system produces smaller and more monodisperse silica nanoparticles. This mixed synthetic route will be discussed later. Some properties of silica nanoparticle include [82–85] easy surface functionalization, [86–89] chemical inertness, low toxicity, light transparency, and good water solubility. These properties have promoted silica-based nanomaterials as potential candidates for engineering hybrid multifunctional nanostructures for biomedical applications [90]. For instance, numerous researchers have created diverse functionalized and doped silica nanostructures through

the Stöber et al. [81] method, inverse microemulsion [91–93], and one-pot synthesis, generally in combination with semiconductor QDs, metallic nanoparticles, organic fluorescent dyes, functional molecules, and drugs as doping agents [94–97]; these approaches have resulted in multifunctional fused nanostructures with multiple morphologies such as core–shell, multicore–shell, sesame ball, hollow and yolk–shell structures [98], which have exhibited great effectiveness for drug delivery, plasmid cell transfection, and theragnostic applications (Table 3) [99–101].

Mesoporous Silica Nanoparticle Synthesis and Applications

In recent decades, many clever efforts have been made to improve and exploit the unique physicochemical properties of silica, which has been reflected in an exponential increase in the number of distinct applications. In this context, some mesoporous silica nanomaterials have emerged from the combination of various synthesis methods, particularly combining solgel chemistry with templating methods by using cationic, anionic surfactants and triblock copolymers as templates [109–111]; these methods generally yield diverse zero-dimensional, one-dimensional, two-dimensional, and three-dimensional (3D) mesoporous nanostructures that exhibit unique physicochemical properties such as high thermal stability, resistance to corrosion, large surface area, ordered pore structure, easy surface functionalization, and tunable pore volume and particle size. It is worth mentioning the pioneering work by Mobil researchers [112], who produced ordered hexagonally mesoporous nanostructures called MCM-41 through a surfactant-templated procedure assisted by hydrothermal treatment and further calcination. Similarly, Zhao [113] created well-ordered hexagonal mesoporous silica structures called SBA-15 through triblock copolymer synthesis (PEO-PPO-PEO) using amphiphilic block copolymers and the cationic surfactant cetyltrimethylammonium (CTA+) under acidic conditions as organic structure-directing agents (organic templates). Depending on the synthetic method used, complementary steps are required to develop mesoporous nanomaterials, for instance, by removing the surfactant template through calcination, acidic washing, or solvent extraction. Inherently, the governed self-assembly interaction and the reaction conditions (e.g., surfactant concentration, silica precursor, pH, and temperature) can control the morphology, surface area, and pore size and volume.

Mesoporous silica materials can be synthesized with diverse morphologies and mesostructures. The very well-known M41S family, for example, consists of diverse geometric structures (e.g., MCM-41, MCM-48, and MCM-50) that, in conjunction with SBA-15, are typical mesoporous silica materials, which have 2-hexagonal honeycomb-like porous structures, 3D-cubic structures, and lamellar structures [114]. Regarding the morphology, mesoporous nanostructures with different geometries have been produced, including hollow spheres, rods, gyroids, fibers, and helical fibers, which have been associated with the fine control of the reaction system [98]. A variety of synthetic routes for mesoporous silica nanoparticles have been proposed. The most common synthesis techniques are based on the modified Stöber method and on the soft template method, which produce hollow silica materials employing various soft templates such as amphiphilic surfactants, micelles, microemulsion droplets, and vesicular structures. On the other hand, the hard template method has also been used. This method is based on the use of polymer beads such as polystyrene (PS) particles and metal or oxide nanoparticles. Finally, an aerosol-assisted synthesis method has also been described [115].

The unique characteristics of mesoporous silica (i.e., large surface area, pore diameters usually from 2 to 50 nm, and surface functionalizability) are the driving force for interesting catalysis, adsorption, and sensing applications. These important properties have allowed the synthesis of silica hybrid nanostructures for drug

Table 3 Diverse synthesis routes for silica nanoparticles and their applications

Synthesis method	Biosensing/theragnostic	References
Solgel	Chemically reactive surface and FITC encapsulation for potential bioimaging device	[102]
Modified Stöber	Fluorescent silica nanoparticle for high-resolution STED and confocal microscopy	[103]
Modified Stöber	Fluorescent silica nanoparticles for cervical cancer cell line imaging	[85]
Inverse microemulsion	Gene delivery	[104]
Modified Stöber	Chemical sensing	[105]
Ultrasonication solgel	Drug delivery and gene delivery	[106]
Modified Stöber	Targeted cell imaging	[107]
Inverse microemulsion	Leukocyte counting with a sheath-flow-free microchip flow cytometer	[108]

delivery with increased loading and release rates, combining fluorescent and therapy molecules, and these hybrid systems have been used for catalysis and sensing recognition (Table 4) [116–118]. The use of hybrid mesoporous silica nanomaterials has improved current DDSs based on pure silica materials [119–122]. The motivation behind the development of these hybrid nanosystems is founded on the fact that the pore tunnels of mesoporous silica can be loaded with anticancer drug molecules and fluorescent contrast agents and then arranged dynamically by sealing the pores through stimuli-responsive supramolecular interactions employing matching molecules, or even nanoparticles, which can act as "gatekeepers." The on-demand open–close response of such gatekeepers can be achieved by using either exogenous stimuli such as light, temperature, electricity, or magnetic field or endogenous stimuli such as pH gradients, enzymes, and temperature changes. In this way, systems with true control over the drug release kinetics are obtained [115, 123–129].

Recently, some authors have gone beyond the limits of common morphologies of mesoporous silica nanoparticles (e.g., hollow spheres, fibers, rods, and spherical nanoparticles) due to their inherent limitations in surface area accessibility, which significantly diminishes the loading capacity of molecules of interest. Typically, mesoporous silica nanostructures are limited to small molecule cargo due to the uncontrolled synthesis of materials with large pore sizes [137]. Thus, to overcome this limitation, engineered dendritic silica particles have recently been fabricated. For instance, Polshettiwar et al. [138] synthesized fibrous silica nanospheres (KCC-1) using cetylpyridinium bromide (CPB) or cetyltrimethylammonium bromide (CTAB) as templates and a microwave-assisted hydrothermal technique. The nanospheres showed a high surface area produced by the dendritic silica fibers as well as advantageous thermal, hydrothermal, and high mechanical stabilities that can be used for extended applications [111, 139, 140]. On the other hand, 3D-dendritic mesoporous silica nanospheres that contain a center-radial mesostructure have also been produced by chemical methods. The synthesis was achieved by using the biphase stratification method. This synthetic route can control the large pore size and thickness of mesoporous nanospheres, which were successfully confirmed to be protein-releasing nanocarriers. In addition, this synthesis method allowed the construction of uniform mesoporous core–shell nanostructures with Au nanoparticles and Ag nanocubes as cores with 3D dendritic mesoporous radial channels [111, 141, 142]. These silica nanostructures exhibited a high surface area and an increased protein loading capacity due to control of the structural characteristics through tuning of the particle size, pore size length, and thickness. The physicochemical properties of these materials suggest their feasibility for multiple useful applications [143–146].

Carbon Dot–Silica Nanoparticle Synthesis and Applications

One of the first approaches regarding the combination of carbon/silica gel was carried out in 1998 by Nobosuke et al. [147] [148]. By using polycyclic aromatic compounds as graphite precursors, the solgel method and calcination, the authors produced a carbon/silica gel nanocomposite that showed interesting photoluminescence properties. They suggested that the carbon contained within the nanocomposite was the key factor regarding the green luminescence, while the blue luminescence was generated by the silica gel matrix. The authors concluded that the pi-electron conjugated system and the photoluminescence required further study. To the best of our knowledge, Nobosuke's study was pioneering in the production of fluorescent carbon/silica nanocomposites. Currently, there are variations in the fabrication methods of carbon/silica nanocomposites, principally because the source of fluorescent carbogenic elements is now provided by CDs, which can be presynthesized separately. Moreover, new variations have been achieved through distinct synthesis techniques, where the CDs have been grafted or doped

Table 4 Diverse synthesis routes for mesoporous silica nanoparticles and applications

Synthesis method	Biosensing/theragnostic	References
Modified Stöber	MRI contrast agent and optical sensing for in vivo and in vitro applications	[130]
Modified Stöber	Tumoral LNCaP cells selectivity and internalization	[131]
Modified Stöber	Nanotheranostics for camptothecin delivery and multimodal imaging	[132]
Modified Stöber	Drug delivery and hyperthermia	[133]
Modified Stöber	Removal of sodium dodecylbenzenesulfonate	[134]
Modified microemulsion assisted by the diffusion of metal precursors	Potential application for catalysis, optics, or nanomedicine	[135]
Single-micelle templating	Antimicrobial applications	[136]

in a silica matrix, forming a single nanostructure. In the following sections, we review some of the most interesting methods proposed for the synthesis of CD–silica hybrid nanostructures.

Recently, most of the strategies focusing on producing nanocomposites or nanoparticles of carbon/silica have used CDs and silica precursors [149, 150]. The most commonly used synthesis method involves the combination of various techniques, for example, the typical synthesis of mesoporous silica plus the addition of presynthesized CDs. In some cases, CDs can be synthesized in situ with mesoporous silica [151–153]. For the creation of multifunctional CD–silica nanoplatforms, it is highly important to design a suitable functionalization and bioconjugation strategy to obtain successful interactions and good results in theragnostic, biomedical, and sensing applications [53, 57, 67], given that mixing two distinct nanoparticles and linking with other different components (reactive groups, organic and inorganic components, and biomolecules) requires good knowledge of conjugation chemistry, click chemistry, and supramolecular chemistry. Engineering a suitable linking strategy depends on the intended objective and the order of the involved components. In this case, silica is the best candidate for functionalization due to its facile surface chemistry and capacity to assemble a few layers through the linkage of silane coupling agents. Many silane coupling agents exist, and some of the agents most commonly used in theragnostics and biosensing include (3-aminopropyl)trimethoxysilane (APTMS), (3-aminopropyl) trimethoxysilane (APTES), 3-mercaptopropyltrimethoxysilane (MPTMS), 3-(trihydroxysilyl)propyl methylphosphonate monosodium salt solution (THMPS), and TMOS. Some of these siloxane precursors not only grant functional groups to facilitate functionalization or bioconjugation but also, in some cases, can serve as colloidal stabilizers [154–158].

CD–silica nanostructures have attracted the interest of the scientific community, especially materials scientists, since combining CDs with silica in a single hybrid functional nanostructure results in a novel smart approach to exploit the physicochemical properties of both materials concomitantly for different potential applications (Tables 5 and 6) [159–165].

Molecular Imprinting Technique

The molecular imprinting technique (MIT), which produces molecularly imprinted polymers (MIPs), is a synthetic process that involves host–guest supramolecular systems. This technique is based on the bonding of a polymer (host) to a target molecule (guest). The target molecule interacts either covalently or noncovalently with specific functional groups from the host–polymer matrix; subsequently, the target molecule is removed from the polymer, creating an interacting cavity or template, which is then able to rebind a new guest target molecule when the MIP is mixed with a sample that contains the target molecule [174, 175]. There are three typical synthesis routes to obtain MIPs: (i) synthesis from monomers in the presence of a template, (ii) phase inversion; and (iii) soft lithography. MIPs can be applied for biomarker sensing, pathogen detection, and nonsensing applications such as chiral molecule detection, catalysis, and specific separation processes [176, 177]. Recently, numerous approaches have been developed to fabricate multipurpose nanoplatforms by using the MIT combined with fluorescent signal molecules or targeting molecules. Additionally, engineered MIPs have been used as molecular recognition sensors of different analytes such as biomolecules, ions, and chemical and biological moieties [178, 179]. For example, Amjadi and Jalili [180] prepared a multiemission mesoporous multilayered structure constituted by semiconductor QDs, CDs, and silica shells. The employed route to obtain the materials was performed through a one-pot method assisted by the Stöber solgel synthesis and MIT. The preparation of the nanoprobe was carried out as follows: Previously synthesized carbon QDs were covered with a layer

Table 5 Diverse synthesis routes for silica–CD nanoparticles and biosensing applications

CD synthesis method	Synthesis method for silica–carbon nanoparticles	Biosensing/theragnostic	Refs.
Organosilane pyrolysis	Organosilane pyrolysis	Vanadium(V) detection	[166]
One-pot solvothermal	One-pot solvothermal	Fe3 + detection and cancer/normal cell differentiation	[167]
Organosilane pyrolysis	Stöber/molecularly imprinted silica	Sensing of rhodamine 6G	[168]
Microwave irradiation	Reverse microemulsion	Photocatalyst for highly selective solar fuel production from CO_2	[169]
One-pot copolycondensation/solgel	One-pot copolycondensation/solgel	Temperature sensing and cell labeling	[170]
Hydrothermal	Solgel	Cu2 + ion detection	[171]
Organosilane pyrolysis	Solgel	Nitride sensing in food	[172]
One-step hydrothermal method	Solgel/molecularly imprinted silica	Anti-inflammatory drug celecoxib detection	[173]

Table 6 Diverse synthesis routes for hybrid carbon dot/silica/magnetic nanoparticles and bioapplications

CD synthesis method	Synthesis method for magnetic nanoparticles	Synthesis method for silica–magnetic nanoparticles	Biosensing/theragnostic	References
Organosilane pyrolysis	High-pressure hydrothermal	Solgel/surfactant template	Potential bioimaging sensor	[253]
Hydrothermal	Solvothermal method	Solgel/surfactant template	Drug delivery, fluorescence, and MRI	[230]
Hydrothermal	Coprecipitation method	Solgel	Fluorescence sensing, magnetic separation, and live cell imaging of fluoride ions	[254]
Hydrothermal	Solvothermal method	Reverse microemulsion/molecularly imprinted polymer	2,4,6-Trinitrophenol (TNP) detection	[255]
Calcination	Calcination	Solgel/surfactant template and calcination	Fluorescence and magnetic contrast agent for in vivo and in vitro applications	[130]
Diverse synthesis routes for hybrid carbon dot/silica/gold nanorod nanoparticles and bioapplications				
CD synthesis method	**Synthesis method for gold nanorods**	**Synthesis method for silica-gold nanorods**	**Biosensing/theragnostic**	**Reference**
One-step hydrothermal method	Seed-mediated growth method	Solgel	Atherosclerosis detection	[256]

of silica; later, by cocondensation, a layer of mesoporous silica was formed on the layer that covered the carbon QDs. In this step, diniconazole (DNZ), organic QDs, and CTAB were added, with the last reagent added to make the layer porous. Finally, the DNZ and CTAB templates were removed by washing with water and methanol (see Fig. 1a). The authors obtained spherical nanoparticles that showed a rough surface, as observed by scanning electron microscopy (SEM). Similarly, transmission electron microscopy (TEM) analysis revealed nanoparticles with diameters of 100 ± 10 nm (see Fig. 1b). Due to the multiple emission at 470 nm and 530 nm conferred by both QDs, the nanoparticles were used as a ratiometric sensor for the recognition and detection of DNZ, analog molecules and real samples of DNZ in soil, water, and wastewater. To test the sensor behavior, the probe performance was evaluated at different pH values, observing that within the pH range of 6.0–9.0 without analyte, the intensity ratio was not altered, while in the presence of DNZ and at pH 8.0, the intensity ratio was changed. Therefore, the fluorescence intensity showed high sensitivity to DNZ concentration, with a good linear relationship. To understand the relation of fluorescence quenching as a function of DNZ quantity, the binding kinetics of the template were tested versus time. The authors suggested that the higher adsorption of DNZ on the nanoprobe was due to the greater number of recognition sites generated on the pores of the mesoporous shell. These recognition sites were able to rebind the DNZ molecules. Therefore, the authors described that the fluorescence quenching behavior was related to the influence of the functional amine groups that act as acceptors for photogenerated holes in QDs [181, 182]. To verify the efficiency of the sensor, it was compared to common detection techniques, exhibiting a detection limit equivalent to that of ELISA and chromatographic assays, high reproducibility, and stability.

Concerning environmental issues, the combination of mesoporous silica and CDs as hybrid nanomaterials has been employed as a versatile alternative to detect diverse ambient molecules and compounds harmful to human health [153, 178, 183–186]. Clearly, the high quantum yield, low cytotoxicity, tunable fluorescence, high surface area, tunable pore size, and mesoporosity are the outstanding properties exploited to construct these nanosensors. For instance, Liu et al. [187] addressed the detection of bisphenol A (BPA), an endocrine-disrupting organic molecule found in food packaging. In particular, the nanomaterial was obtained by using a MIT and in situ hydrothermal synthesis; the CDs were synthesized through a pyrolysis decomposition method using anhydrous citric acid and AEAPMS as the precursor source. Since MIP-coated CDs were fabricated by solgel synthesis in the presence of a BPA template, TEOS and APTES were used to generate BPA binding sites for recognition. The templates were then removed by the solvent elution method with water/ethanol. In a simple manner, the authors created a highly specific BPA nanosensor, whose sensing principle was based on the fluorescence quenching of CDs, with a reliable concentration sensitivity of 100 nM to 4200 nM and nonspecific detection of interfering ions and phenolic compounds. The nanosensor results were comparable with high-performance liquid chromatography (HPLC) detection and showed a similar extrapolated performance when real river water samples were analyzed.

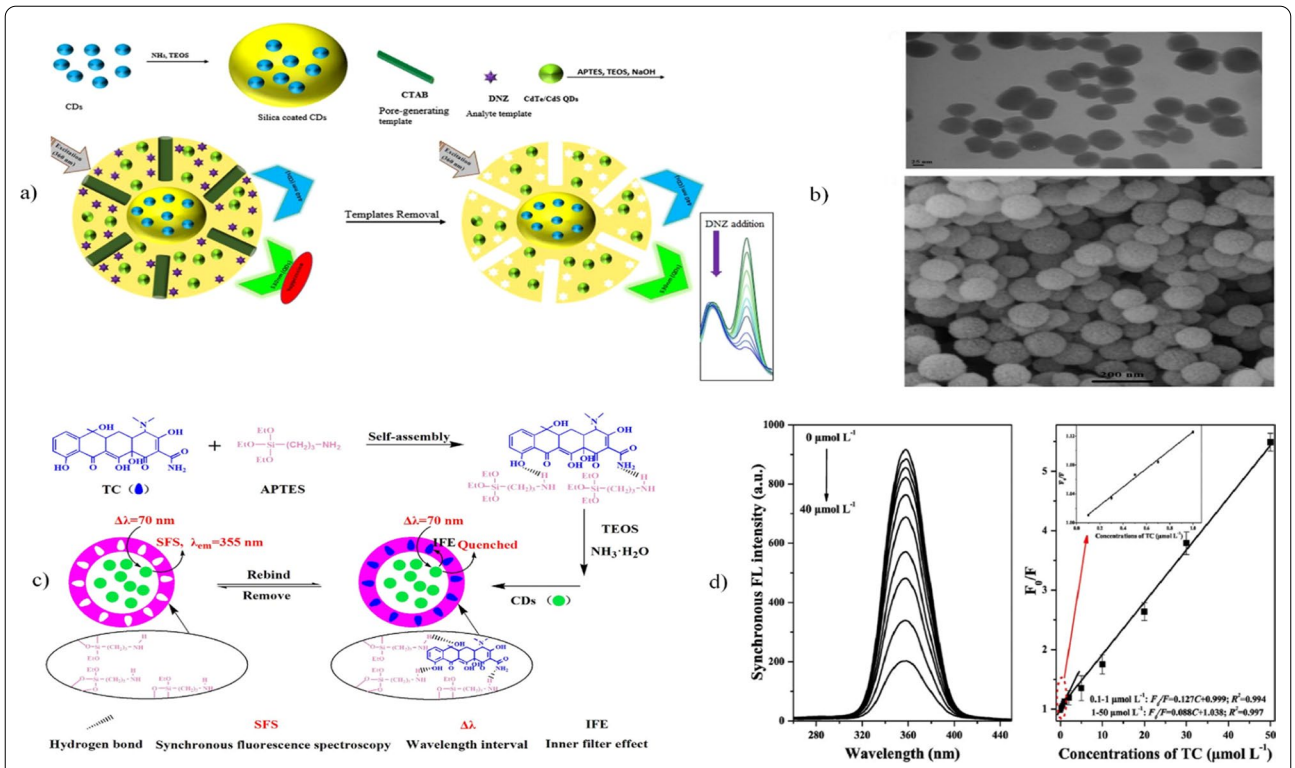

Fig. 1 Representative schemes for the construction and function of CD–silica nanosensors: **a** Scheme of nanosensor construction and operation for diniconazole detection, **b** SEM and TEM micrographs of the mMIP@CDsQDs. Adapted with permission from ref. [180] copyright 2017 Elsevier. **c** Scheme of nanosensor construction and operation for tetracycline detection, **d** SFS spectra showing the fluorescence intensity behavior as a function of the TC concentration. Adapted with permission from ref. [188] copyright 2017 Elsevier

Another similar study was reported by Yang et al. [188]. First, through hydrothermal synthesis, they obtained nitrogen-doped CDs by using citric acid and urea as precursors, and then, a modified inverse microemulsion system (cyclohexane/n-hexanol/Triton X-100/water/CDs) was used to encapsulate the CDs by polymerization of TEOS and APTES. Finally, the analyte was added as a template and removed by washing to create the nanostructure MIP@CDs (see Fig. 1c). The regular spherical nanoparticles obtained were applied as sensors to detect the antibiotic tetracycline (TC). Based on synchronous fluorescence spectroscopy (SFS), the fluorescence quenching induced by the compound was investigated. The results suggested that TC is physically adsorbed on the MIP@CDs, producing a quenching effect of the synchronous fluorescence spectra dependent on the concentration of TC. As complementary deductions, due to the minimal change in fluorescence lifetime observed, the quenching mechanism is related to the inner filter effect (IFE) and not Förster resonance energy transfer (FRET) (Fig. 1d).

Due to their high surface area, pore volume, surface functionalization, and relatively thick wall, mesoporous nanomaterials have been used for gas sensing [189]. Ordered mesoporous materials allow the effective hosting of diverse molecules. For example, Wang et al. [190] obtained a feasible oxygen sensor by grafting CDs in hollow mesoporous silica microspheres (HMSMs), as well as in mesoporous silica microspheres (MSMs). Briefly, anhydrous citric acid and the silane coupler KH-602 were used as precursors for the formation of CDs through the pyrolysis method [190]. On the other hand, MSMs were synthesized by using the surfactants CTAB, tetradecyltrimethylammonium bromide (TTAB), stearyltrimethylammonium bromide (STAB), and triethanolamine (TEA) as cotemplates and TEOS as a polymerizing agent. The process was completed by autoclaving at 383 K and subsequent calcination at 823 K to remove the templates. To fabricate HMSMs, first, PS microspheres were fabricated using polyvinylpyrrolidone (PVP), α,α'-azodiisobutyramidine dihydrochloride (AIBA), and styrene through heating in a water bath. PS microspheres were added to a mixture of TEOS, CTAB, TTAB, ethanol, and ammonium hydroxide, which acted as a basic catalyst. Then, the mixture was heated and calcined at 823 K. Finally, the produced

HMSMs were loaded with CDs for further testing (see Fig. 2a1). The size and shell thickness of the obtained HMSMs were dependent on the surfactant concentration and ratio; moreover, the surfactants CTAB and TTAB, used as structure-directing agents, tended to increase the pore number and particle size (see Fig. 2a2 and a3). The dependence of the fluorescence intensity of loaded CDs-MSMs and CDs-HMSM as a function of analyte concentration was exploited for oxygen sensing; the results suggested that the emission intensity is oxygen concentration dependent, showing a decrease in intensity with higher oxygen concentrations because of a quenching effect. Significantly, the probe showed a response and recovery emission intensity behavior, validated by the nitrogen–oxygen replacement mechanism; additionally, the hybrid nanostructures exhibited a short response time and recovery time of 4.85 and 23.23 s, respectively, which are desirable for oxygen sensors (see Fig. 2b).

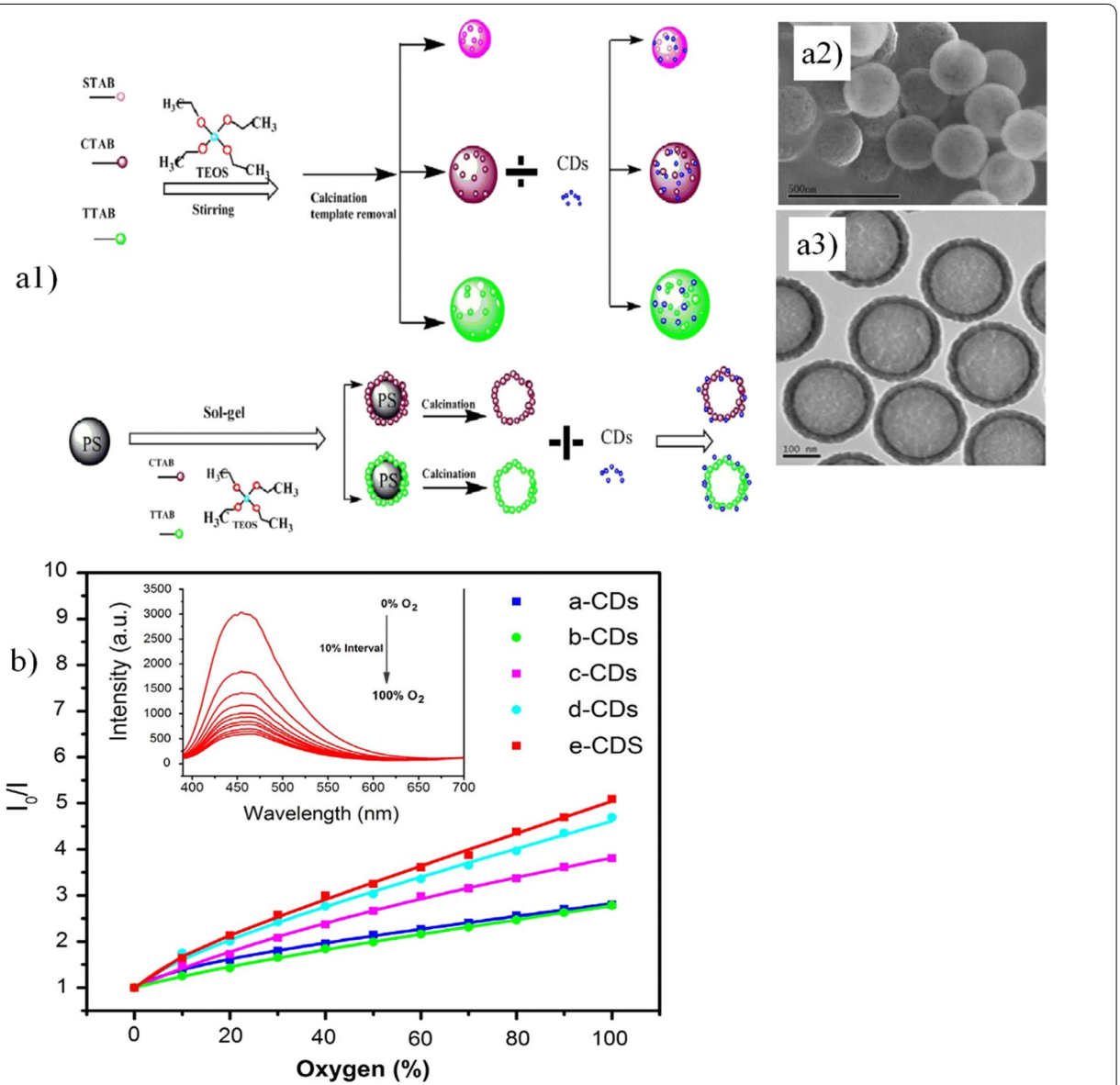

Fig. 2 **a1** Scheme of the construction of the nanosensor for oxygen sensing, **a2**, **a3** FE-SEM and TEM micrographs showing the morphology of the nanoparticles, **b** graph presenting the variation in fluorescence intensity as a function of the concentration of oxygen, and Stern–Volmer plot showing the quenching degree of the luminophore. Adapted with permission from ref. [190] Copyright 2016 Elsevier

Carbon Dot–Silica Nanoparticles by Inverse Microemulsion

In 1981, the term "microemulsion" was defined as a system of water, oil, and an amphiphile that altogether is a single optically isotropic and thermodynamically stable liquid solution [191]. In recent years, diverse descriptions of microemulsions have been reported by chemists, physicochemists, and engineers. The microemulsion formulation is related to the intrinsic physicochemical characteristics that dictate the multifactorial requirements to form a stable microemulsion system [192], which is typically composed of a ternary system (water/oil/surfactant) or quaternary system (water/oil/cosurfactant (usually short-chain alcohols)/surfactant) [193]. Regularly, microemulsions form spontaneously, and they exhibit thermodynamic stability because the free energy of the microemulsion is lower than that of the separated states [194]. In a microemulsion system, primarily, the surfactant molecule is adsorbed at the oil–water interface, reducing the interfacial tension and conferring stability to the dispersed phase. In microemulsions, the self-assembly of surfactant molecules produces discrete surfactant aggregates that are topologically diverse (i.e., spherical micelles, cylindrical micelles or rodlike, vesicular, lamellar, and reverse micelles) [195, 196]. The shape and size of these supramolecular structures depend on multiple factors such as the hydrophilic–lipophilic balance (HLB), critical micellar concentration (CMC), and surfactant packing parameter ratio ($N_s = v/al_c$) [197–199]. These aggregates are in the nanosize range and can be exploited as nanoreactors. Specifically, reverse micelles or inverse microemulsions have been used as nanoreactors or "water pools" for the synthesis of various nanomaterials such as QDs and metallic and polymeric nanoparticles [200–205]. Usually, two reactants are placed in separated microemulsion systems; then, both microemulsions are combined, causing droplet collision and fusion and, later, fission, intermixing the reactants. Afterward, the reaction occurs inside the nanoreactor or water pool [206]. The radius of the water pool can be controlled by varying the water/surfactant ratio, W_0, which allows the synthesis of monodisperse nanoparticles and represents a suitable option to control the particle size because the compartmentalized nanodroplets limit the nucleation, growth, and coalescence aggregation of as-synthesized nanostructures [207]. Silica nanoparticles can be produced with inverse microemulsions, with smaller sizes (below 100 nm) than those obtained by the Stöber method [208–214].

The robust intrinsic properties of CDs, such as high photochemical stability, low toxicity, high quantum yield, and electron acceptor or donor ability, make them potential candidates to detect metallic analytes [166, 215–218]. For instance, Qiao et al. [219] exploited these properties, developing enhanced fluorescence CD–silica nanoparticles to detect cupric ions (Cu^{2+}). The authors produced doped silica nanoparticles with CDs through a one-pot synthesis. First, the passivated CDs were obtained by a hydrothermal pyrolysis technique by using citric acid and PEI as precursors, while to produce doped silica nanoparticles, a solution of PEI-passivated CDs was added to a tailored inverse microemulsion system of TX-100/cyclohexane/1-hexanol/ultrapure water, followed by the addition of TEOS and ammonium hydroxide to the system. The investigation showed interesting results about CD quantum yield improvement. The addition of PEI to the system was intended to graft or cargo the CDs into the silica matrix through supramolecular interactions between PEI amino groups and CD carboxyl groups. The results demonstrated that an optimized PEI concentration not only helped to incorporate the CDs into the silica but also improved the fluorescence quantum yield from 13.7% in free-state CDs to 38.6%. The authors suggested that the possibly improved fluorescence was attributed to the interaction of positively charged tertiary amine groups present on PEI molecules with negatively charged SiO^- groups, while the primary and secondary amines were concentrated and directed to the surface CDs facilitating the supramolecular interaction between carboxyl groups and amine groups (see Fig. 3a). As the authors noted, fluorescence enhancement is due to the aforementioned supramolecular interactions; thus, they used this behavior to create a fluorescence turn-off system by disrupting these interactions with metallic analytes. The results showed that the doped silica nanoparticles have higher selectivity for detecting copper ions since they can form complexes with the amine groups, thereby destroying supramolecular interactions and resulting in a decrease in fluorescence intensity (see Fig. 3b).

Regarding CDs used for biorecognition, various strategies have been exploited [77, 167]. The fluorescence versatility combined with the well-documented silica chemistry allows the creation of nanomaterials for specific biodetection purposes [220–222]. Wu et al. [223] prepared CD-doped functionalized silica nanoparticles to detect alpha-fetoprotein, a glycoprotein related to liver diseases. CDs were obtained through the hydrothermal synthesis of citric acid and ethylenediamine. Then, the fluorescent dots were encapsulated in a silica shell by using an inverse microemulsion system, with TMOS, 3-(trihydroxysilyl)propyl methylphosphonate (THPMP), and APTMS used as polymerizing agents (see Fig. 3c and d). THPMP was added to provide negatively charged phosphate groups, avoiding colloidal instability or agglomeration, while APTMS was used to graft positively charged amino groups as active binding sites. Subsequently, these nanoparticles

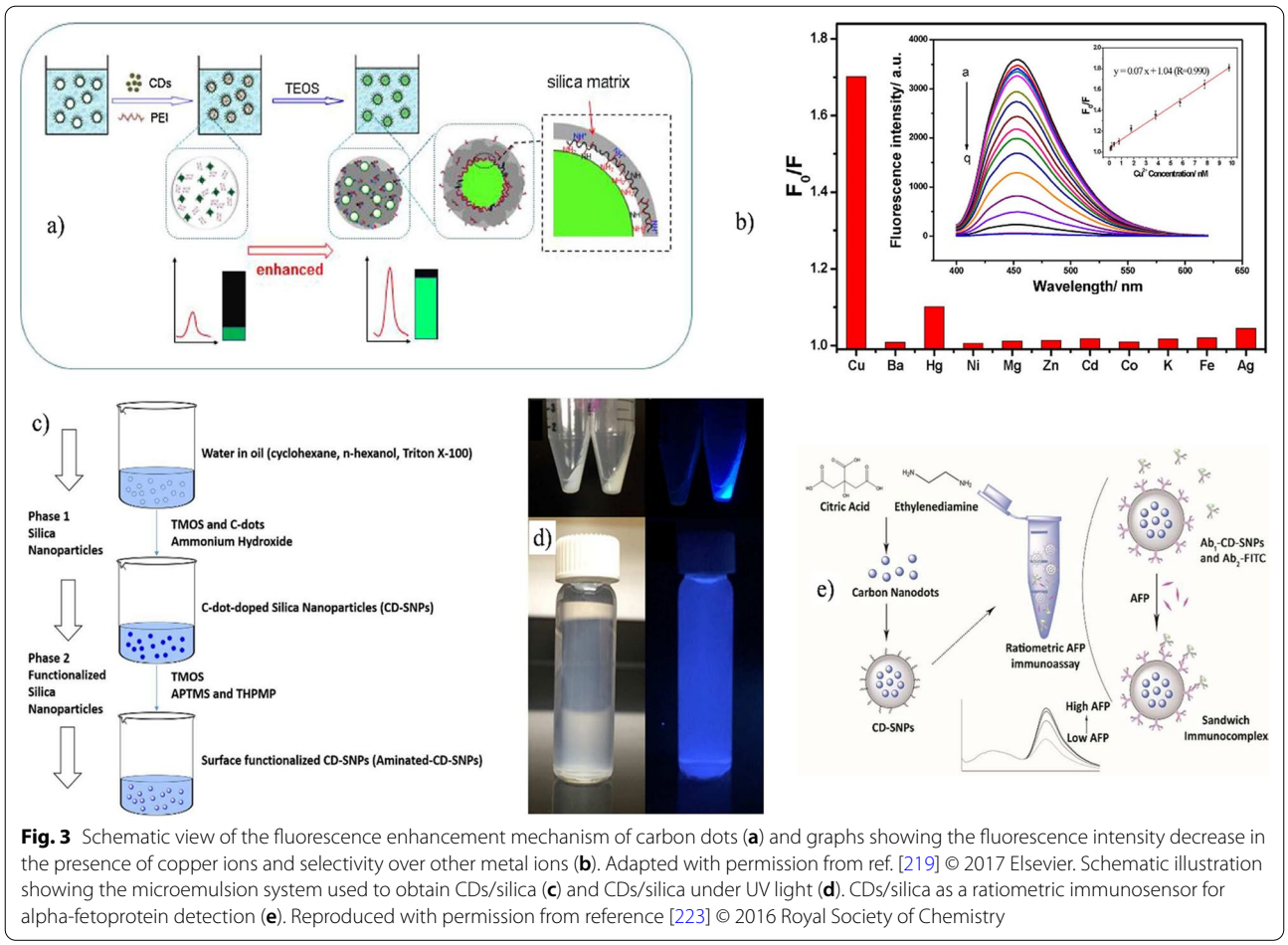

Fig. 3 Schematic view of the fluorescence enhancement mechanism of carbon dots (**a**) and graphs showing the fluorescence intensity decrease in the presence of copper ions and selectivity over other metal ions (**b**). Adapted with permission from ref. [219] © 2017 Elsevier. Schematic illustration showing the microemulsion system used to obtain CDs/silica (**c**) and CDs/silica under UV light (**d**). CDs/silica as a ratiometric immunosensor for alpha-fetoprotein detection (**e**). Reproduced with permission from reference [223] © 2016 Royal Society of Chemistry

were covalently bonded to anti-alpha-fetoprotein through glutaraldehyde cross-linking to build an $Ab_1 - CD - SNPs$ component, which was later mixed with a second component of secondary anti-alpha-fetoprotein $Ab_2 - FITC$, forming an immunocomplex. The immunosensor showed dual emission at 440 and 550 nm, with the first peak due to the CDs and the second from FITC. This multiemission system was successfully used to detect alpha-fetoprotein, obtaining a good linear relationship of 0.317–280 μg/dl with a correlation of $R^2 = 0.997$ (see Fig. 3e).

Concerning the nanomedicine field, several researchers have created distinct nanomaterials for applications in biological systems. Fluorescent, magnetic, polymeric, and metallic nanoparticles have been used for bioimaging, drug delivery, and therapy. In this sense, the nanoparticles can be combined with organic and inorganic moieties to form theragnostic nanoplatforms [151, 224–229]. Some of these nanoplatforms have been a hot research topic in nanomedicine because of their improvement in diagnosis and therapy in biological system applications (Table 6).

For instance, Das et al. [230] developed a theragnostic nanoplatform that exploits the intrinsic properties of nanomaterials, such as superparamagnetism, high fluorescence, mesoporosity, and high surface area [231]. Based on supramolecular interactions, they developed a host–guest system capable of assembling different nanomaterials. The prepared nanoplatforms were obtained through diverse synthesis and assembly steps. First, magnetic gadolinium and iron oxide nanoparticles were synthesized by a solvothermal method. Then, through the cationic surfactant CTAB and the polymerizing agents TEOS and APTS, the magnetic nanoparticles were coated with silica layers, creating a core–shell structure. Later, the nanoparticles were functionalized with positively charged amine groups, which served to bind negatively charged boronic acid-functionalized CDs (BNSCQDs) that had been previously synthesized [79].

This nanoplatform was able to modulate various engineered functions for cancer cell detection and treatment (see Fig. 4a). In this context, the silica shell adsorbed the chemotherapeutic drug and served to graft the BNSCQDs, which acted as pH-dependent gatekeepers that

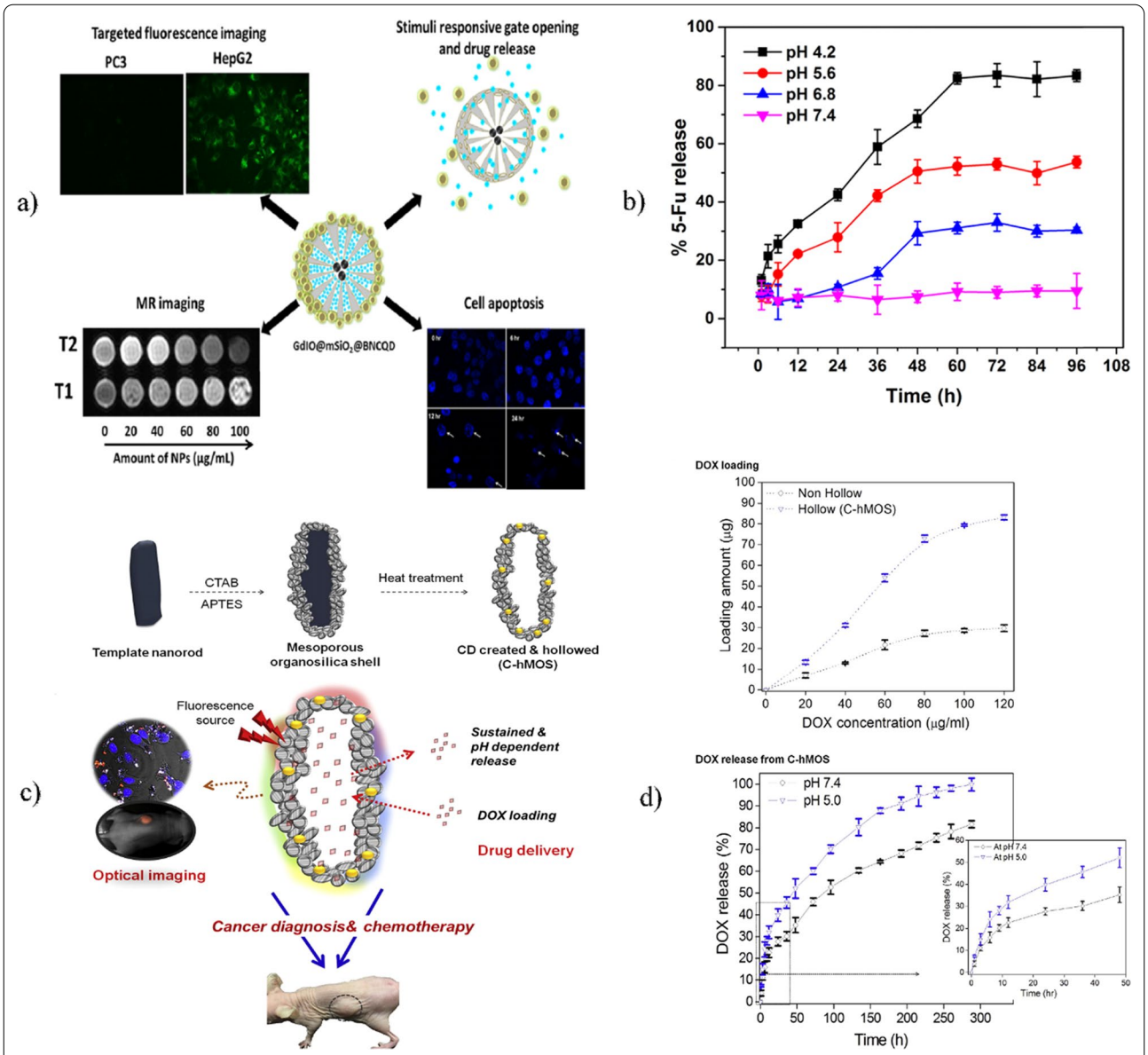

Fig. 4 Schematic representation of multifunctional nanoplatform construction for theragnostic applications. **a** Hybrid nanoplatform composed of a core of magnetic gadolinium oxide nanoparticles coated with silica and charged with 5-fluorouracil and carbon quantum dots functionalized with boronic acid as a lid. **b** Graph of drug release at different pH values. Adapted with permission from ref. [230] © Copyright 2018 Elsevier. **c** CD/hollow nanoparticles used for drug delivery and bioimaging. **d** Graph of drug loading and pH-dependent release [151] © Elsevier 2017

allowed controlled loading and release of the drug, as well as the generation of multifluorescence emission in the range of 370–500 nm, which played an important role in monitoring the interaction of the nanoplatform with the cells. On the other hand, the magnetic nanoparticles granted outstanding relaxivity values of $r_1 = 10\ \mathrm{mM^{-1}s^{-1}}$ and $r_2 = 165\ \mathrm{mM^{-1}s^{-1}}$ measured by a clinical MRI scanner. The nanoplatform was successfully used for in vitro HePG2 cell detection through the overexpressed sialyl Lewis^a (SL^a) receptor. Additionally, the nanoplatform was successfully used for the release of the drug 5-fluorouracil. To validate the release mechanism, the nanoplatform was subjected to different pH values, showing an optimal percentage of initial release of 13% in 12 h and a final value of 85% in 60 h at a pH of 4.2 (see Fig. 4b). Notably, this work opened a new potential application of CDs combined with diverse nanomaterials, creating an engineered advanced theragnostic device for nanomedical applications [230]. Kang et al. [151] reported the development of CD hollow mesoporous

organosilica nanocarriers (C-hMOSs) [170, 232]. The procedure was achieved through the precipitation reaction and surfactant-templated method in the presence of CTAB. The precipitation reaction produced hydroxyapatite (HA) nanoparticles, which were implemented as a core template to create a hollow structure. To fabricate the hollow mesoporous nanoparticles, first, a nonhollow silica structure was synthesized through a modified base-catalyzed solgel process to coat the core template nanoparticles via polymerization of TEOS and APTES. The fluorescent CDs were generated by heating the nonhollow nanoparticles at 400 °C, which were then converted into a hollow-cored structure by removing the core with an acid etching process. The produced multifluorescent hollow-spaced mesoporous silica rods were applied and studied extensively in biological systems (see Fig. 4c). The theragnostic platform showed potential as a drug nanocarrier, in tissue imaging and as a cell marker. To address these capabilities, the nanocarrier was loaded with the chemotherapeutic drug doxorubicin (DOX) and then tested in vitro and in vivo. Interestingly, the nanocarrier exhibited a surface area value of 1087 m^2/g and pore volume of 0.843 cm^3/g, which are favorable for drug loading. To verify the theragnostic properties of the nanocarrier, the HeLa cancer cell line was cultured with different concentrations of the DOX-loaded nanoparticles. The results revealed pH-dependent drug release behavior, with faster release at pH 5.0 than at pH 7.4 (see Fig. 4d). The toxic effects of the nanocarrier to cells were studied based on the expression of caspase 3, which was observed by confocal microscopy. Likewise, the quantification of cells positive for the apoptotic marker was performed through flow cytometry, where values of 66% and 91% were found for free DOX and the nanocarrier loaded with DOX. Moreover, the in vivo performance of the nanocarrier was confirmed in MCF-7 tumor-bearing nude mice that were administered the nanocarrier by intratumoral injection. The nanocarrier showed a fluorescent signal at the tumor location and promoted DNA fragmentation as well as tumor growth suppression [151].

The limitations of the current pharmaceutical formulations for cancer treatment, including antitumor off-target effects, poor solubility, and uncontrolled release, have led to considerable adverse health effects [233, 234]. Thus, there exists an urgent need to improve the efficacy of pharmaceutical treatments because of the high rate of deaths per year associated with cancer [235]. The unique characteristics of materials at the nanoscale facilitate their interaction with biological systems, which allows the above-mentioned issues to be addressed [236–238]. Two of the most exploited biological applications of nanomaterials are bioimaging and drug delivery for cancer therapy [239–246]. Due to their nature, CD–silica nanoparticles can be merged as multimodal nanoplatforms. For example, Liu et al. [247] constructed a versatile nanoplatform that combines some of the properties of different materials. The nanoplatform exploited the photosensitizing properties of Rose Bengal (RB), the high photostability of CDs, and the features of mesoporous silica in a system identified as MSN@C-dots/RB. RB acted as a photosensitizer for photodynamic therapy, CDs acted as a bioimaging agent, and silica served as a carrier for the loading and release of the chemotherapeutic DOX. The nanomaterial was tested against the human lung cancer cell line NCI-H1299 and as a bactericidal agent against *Escherichia coli* (see Fig. 5a). The authors fabricated CDs through a solvothermal method by using dimethylformamide (DMF), urea, and citric acid. Then, the CDs were embedded into mesoporous silica nanoparticles using an oil–water biphasic stratification method, which employed the cationic surfactant cetyltrimethylammonium chloride (CTAC) as a template, TEOS as a silica source, TEA as a catalyst, and 1-octadecene or cyclohexane as the organic solvent. Similarly, the MSN@C-dots/RB nanoparticles were obtained by the same approach adding the photosensitizer RB into the reaction system. During the synthesis, it was observed that at higher doping concentrations of RB or CDs, the morphologies of the nanoparticles were affected; thus, to avoid this drawback, a mesoporous silica shell was epitaxially grown onto the CDs, which produced wormlike morphologies with mesoporous channels that extended to the surface of the nanospheres; these channels increased the loading capacity of DOX and RB. The potential of the nanoplatform for drug delivery and bioimaging was evaluated. First, the increased pore volume, surface area, and mesoporosity caused by epitaxial growth permitted efficient loading of the therapeutic drug and the antibiotic ampicillin into the nanoplatform, which was used for treating the human lung cancer cell lines NCI-H1299 and *E. coli*. The loading and release of DOX were confirmed through pH changes. The percentage of loading was 34.4% (w/w), while the release was pH dependent. A higher percentage of release was reached at pH 5.0, with a percentage value of 50.5%, whereas, for ampicillin, the value was 29.3%. Regarding the optical properties, the MSN@C-dots/RB nanoparticles exhibited excitation-independent photoluminescence and broad emission from 570 to 660 nm. This broad emission was favorable for bioimaging applications. Another highlighted ability of MSN@C-dots/RB was its multifunctionality in chemo/photodynamic therapy. Cells were incubated with the nanoparticles and irradiated at 530 nm and 300 mW cm^{-2} to generate singlet oxygen, $^1O_2$, which reduced the viability of cancer cells in combination with DOX. Moreover, the nanoparticles loaded with the antibiotic and irradiated showed

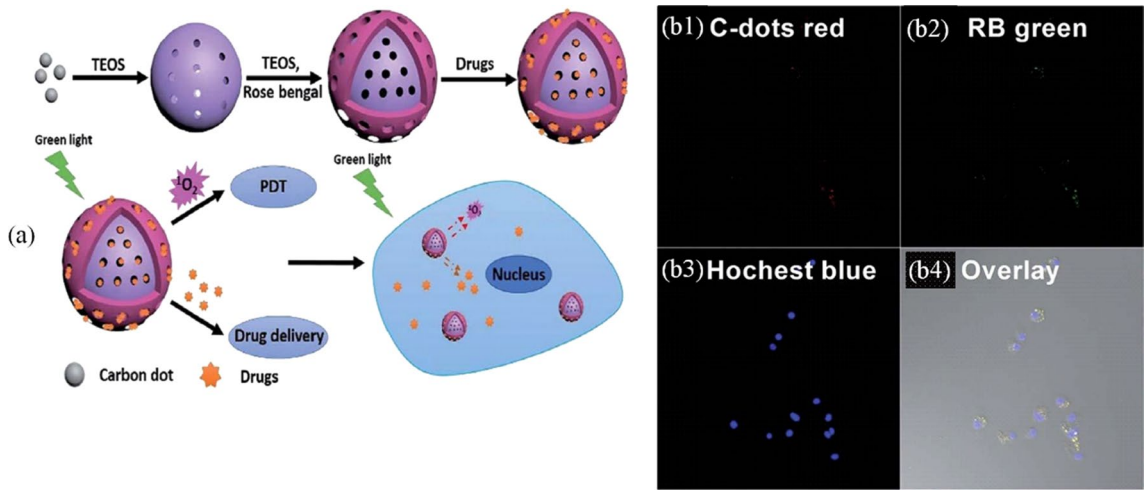

Fig. 5 **a** Schematic representation of the multifunctional nanoplatform of silica–CDs. **b** The nanoplatform is localized in the cytoplasm, and the signal is due to the red CDs. All (**b1**–**b4**) images were obtained by confocal microscopy. Reproduced with permission from reference [247]. Copyright 2017 Royal Society of Chemistry

bacterial inhibition. Additionally, the MSN@C-dots/RB nanoparticles were visualized within the cytoplasm, suggesting that they can be used for monitoring cancer cells (see Fig. 5b1–b4).

Currently, diverse research groups have aimed to design nano-DDSs to improve and guarantee a major degree of drug delivery efficiency [132, 133, 248]. For this purpose, researchers can arrange diverse predesigned organic and inorganic functional molecules to form different nanostructures and identify superior results [249, 250]. This type of nanostructure is dominated by supramolecular chemistry interactions including self-assembly, hydrogen bonding, van der Waals forces, dipole–dipole interactions, hydrophobic interactions, and so forth [251]. Therefore, these interactions are a powerful tool for engineering nanomaterials as "gatekeepers," which can modulate controlled drug delivery. For example, Shirani et al. [252] created a nanocarrier for drug delivery and bioimaging. The nanocarrier traits are conferred by the mesoporous silica and luminescent CDs [252]. In brief, the synthesis was performed by using the pyrolysis route to obtain CDs from glucose and L-aspartic acid. Then, mesosilica-coated CDs (MSCDs) were produced by the solgel process assisted by CTAB and TEOS. Later, the surface of the nanoparticles was modified with APTES to incorporate amine groups. Consequently, to provide multifunctional drug delivery and imaging behavior, the MSCDs were loaded with the antineoplastic agent epipodophyllotoxin (ETO) and conjugated with β-cyclodextrin (C β CD) through an N-(3-dimethylaminopropyl)-N-ethylcarbodiimide hydrochloride (EDC)/N-hydroxysuccinimide (NHS) reaction to form an amide linkage. Finally, FA moieties were attached to the conjugated structure (see Fig. 6a). This nanocarrier was then applied to HeLa and Hep2 cells. The results showed that pH-responsive drug release increased in the acidic microenvironment. Furthermore, the folate-decorated nanocarrier interacted with folate receptors (FRs) targeting cancer cells and promoting cellular uptake, which was observed by fluorescence microscopy due to signals emitted by CDs (see Fig. 6b–d).

Zhao et al. [225] developed a DDS that responds to dual endogenous stimuli such as redox and enzyme stimuli. The nanosystem was produced using CDs-PEI and hollow mesoporous silica. The CDs were synthesized through a hydrothermal method by using citric acid and PEI as starting precursors. Then, functionalized hollow mesoporous silica nanoparticles (HMSN-SH) were prepared by an etching process. In particular, SiO_2 nanospheres were obtained using the Stöber method through TEOS and CTAB and thiol-functionalized by MPTMS. Once the HMSN-SH were obtained, they were further reacted with Py-SS-COOH through a disulfide bond exchange reaction, resulting in modified HMSN-SS-COOH, which was then loaded with DOX and activated with EDC/NHS to covalently graft the positively charged CDs-PEI through an amidation reaction; the final product was obtained after cladding with hyaluronic acid (HA) (Fig. 6e). These HMSN-SS-CD-PEI@HA nanoparticles were used to treat the cancer cell lines A549 and NIH-3T3. The CDs-PEI acted as an imaging agent and played a gatekeeper key role for targeted drug delivery, also conferring controlled drug release. The nanoparticles showed cumulative DOX release at pH values of 7.4

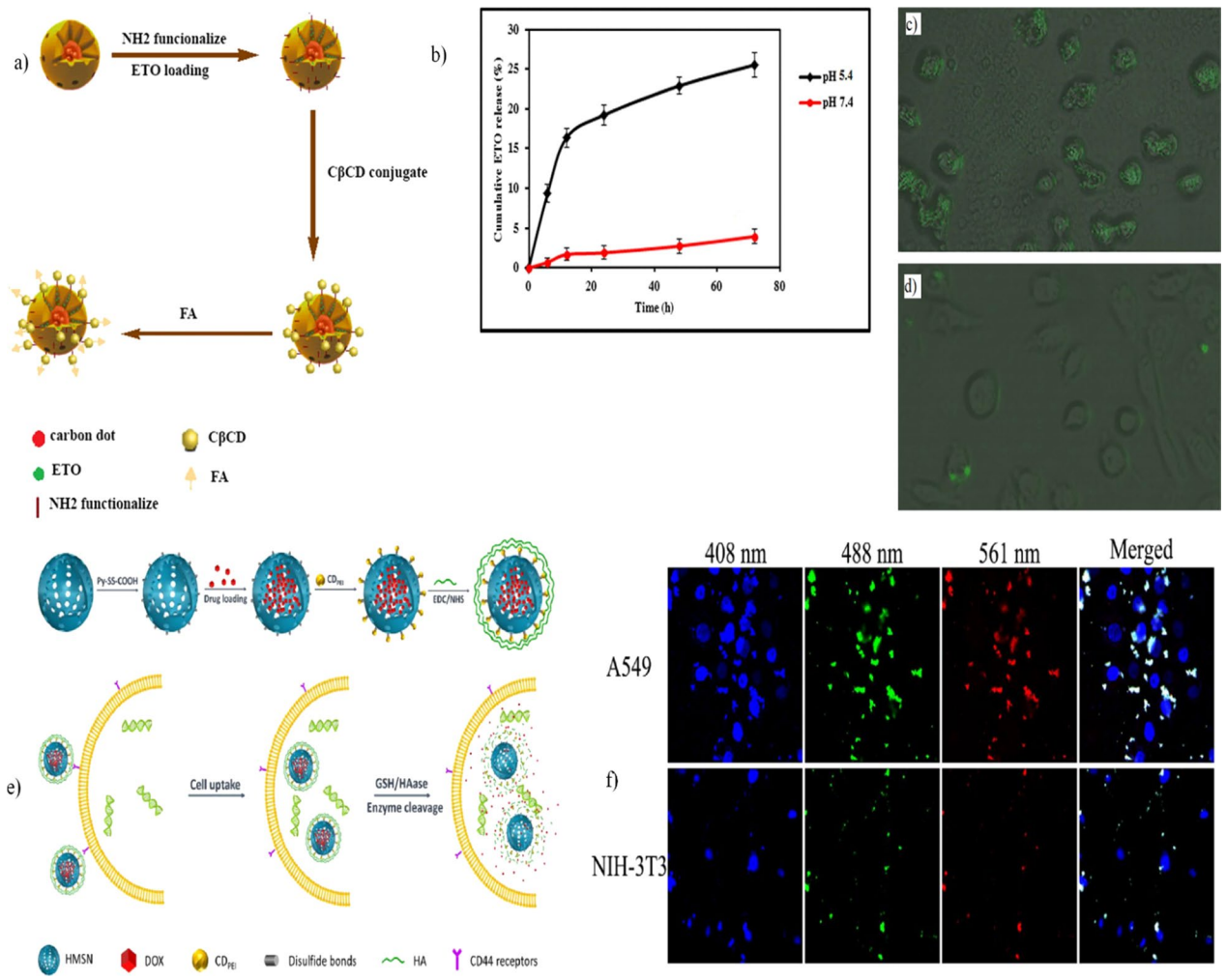

Fig. 6 **a** Scheme of the formation of pH-responsive nanocarriers for drug delivery and bioimaging, **b** graph of drug release at different pH values of 5.4 and 7.4, **c**, **d** fluorescence images of endocytosis of FA-C β CD-MSCD-ETO by HeLa and HepG2 cells. Adapted with permission from ref. [252] © 2018 Elsevier. **e** Schematic representation of nanoplatform formation, drug loading, and the mechanism of dual-stimuli drug release. **f** Endocytosis of the nanoplatform by A549 and NIH-3T3 cells. Images obtained by CLSM. Adapted with permission from ref. [225]. Copyright 2017 Elsevier

and 5.0 due to the influences of high concentrations of glutathione (GSH) present on the tumor cells, suggesting successful redox-responsive behavior enhanced by HAnase. Considerably, the nanosystem showed potential enhanced theragnostic performance assisted by the outstanding CD fluorescence properties and the verified intrinsic drug cargo loading property of mesoporous silica (Fig. 6f) [225].

Conclusions

The outstanding physicochemical characteristics of CDs, silica nanoparticles and their derivatives, either as individual particles or combined as nanocomposites, have attracted increasing interest among researchers of diverse disciplines. Exploiting the eminent characteristics of both nanomaterials combined into one nanostructure has been reflected in improvements and enhanced reliability for potential applications in several science fields. The well-documented synthetic routes and the chemical procedures for functionalization of both nanomaterials facilitate the engineering strategy design for combining and fabricating CD–silica nanostructures. In addition, taking advantage of supramolecular interactions as building blocks to produce hybrid nanostructures allows addressing the current drawbacks of DDSs in biological systems, sensing and biosensing. Smart nanohybrid design (mesoporous silica/magnetic nanoparticles/CDs/cancer active drug or mesoporous silica/plasmonic nanoparticles/CDs/cancer active drug) has opened a new way to exploit the

characteristic physicochemical properties of nanoscale materials in just one nanodevice. The continual search for new synthetic routes to create nanoarchitectures with novel and unique morphologies, such as 3D dendritic mesoporous nanoparticles, will probably lead to more improvements in recent nanohybrids. New studies and more comprehensive knowledge about the photoluminescence mechanism of CDs will surely arise and will permit better control of their luminescence properties. Interdisciplinary work will lead to new insights and reinforce the promising prospects of CD–silica nanostructures as potential nanoplatforms for the discussed applications.

Abbreviations

AEAPMS: N-(β-Aminoethyl)-γ-aminopropylmethyldimethoxysilane; AIBA: α, α'-Azodiisobutyramidine dihydrochloride; APTES: (3-Aminopropyl) triethoxysilane; APTMS: (3-Aminopropyl)trimethoxysilane; BNSCQD: Boronic acid-modified nitrogen, sulfur codoped carbon quantum dots; CDs: Carbon dots; C-hMOS: CD-induced hollow mesoporous organosilica nanocarriers; CTAB: Cetyltrimethylammonium bromide; CTAC: Cetyltrimethylammonium chloride; DDS: Drug delivery system; DNZ: Diniconazole; DOX: Doxorubicin; EDC: N-(3-Dimethylaminopropyl)-N-ethylcarbodiimide hydrochloride; FRET: Förster resonance energy transfer; GC: Gas chromatography; GSH: Glutathione; HA: Hydroxyapatite; HMSMs: Hollow mesoporous silica microspheres; HMSN-SH: Thiol-functionalized hollow mesoporous silica nanoparticles; HPLC: High-performance liquid chromatography; MIP@CDs: Molecular imprinted polymers—carbon dots; MIPs: Molecularly imprinted polymers; MIT: Molecular imprinting technology; MPTMS: 3-Mercaptopropyltrimethoxysilane; MSCDs: Mesosilica nanoparticle-coated carbon dots; MSMs: Mesoporous silica microspheres; NHS: N-Hydroxysuccinimide; PEI: Polyethyleneimine; PEO: Poly(ethylene oxide); PPO: Poly(propylene oxide); PVP: Polyvinylpyrrolidone; Py-SS-COOH: 2-Carboxyethyl-2-pyridyl disulfide; QDs: Quantum dots; SFS: Synchronous fluorescence spectroscopy; SL: Sialyl Lewis; STAB: Stearyltrimethylammonium bromide; TC: Tetracycline; TEA: Triethanolamine; TEOS: Tetraethyl orthosilicate; THMPS: 3-(Trihydroxysilyl)propyl methylphosphonate monosodium salt solution; TMOS: Tetramethyl orthosilicate; TTAB: Tetradecyltrimethylammonium bromide.

Acknowledgements

Not applicable

Author contributions

All authors read and approved the final manuscript.

Author information

Not applicable.

Funding

Not applicable.

Availability of data and materials

Not applicable.

Declarations

Competing interests

The authors declare that they have no competing interests.

Author details

[1]Onkogenetik/Mexicana de Investigación Y Biotectogía SA. de C.V., Av. Miguel Hidalgo y Costilla 1966, Guadalajara, Jalisco, México. [2]Unidad de Biología Molecular, Investigación Y Diagnóstico SA de CV, Hospital San Javier, Pablo Casals 640, Guadalajara, Jalisco, México. [3]Departamento de Clínicas Médicas, Centro Universitario de Ciencias de La Salud, Universidad de Guadalajara, Sierra Mojada 950, Guadalajara, Jalisco, México.

Received: 28 October 2021 Accepted: 4 May 2022
Published online: 04 June 2022

References

1. Toyokazu Y (2018) Basic properties and measuring methods of nanoparticles. In: Naito M, Yokoyama T, Hosokawa K, Nogi K (eds) Nanoparticle technology handbook, 3rd edn. Elsevier, Amsterdam, pp 3–47
2. Balati A, Matta A, Nash K, Shipley HJ (2020) Heterojunction of vertically aligned MoS2 layers to hydrogenated black TiO2 and rutile based inorganic hollow microspheres for the highly enhanced visible light arsenic photooxidation. Compos B Eng 185:107785
3. Balati A, Wagle D, Nash KL, Shipley HJ (2018) Heterojunction of TiO2 nanoparticle embedded into ZSM5 to 2D and 3D layered-structures of MoS2 nanosheets fabricated by pulsed laser ablation and microwave technique in deionized water: structurally enhanced photocatalytic performance. Appl Nanosci 9:19–32
4. Balati A, Bazilio A, Shahriar A, Nash K, Shipley HJ (2019) Simultaneous formation of ultra-thin MoSe2 nanosheets, inorganic fullerene-like MoSe2 and MoO3 quantum dots using fast and ecofriendly pulsed laser ablation in liquid followed by microwave treatment. Mater Sci Semicond Process 99:68–77
5. Polavarapu L, Mourdikoudis S, Pastoriza-Santos I, Pérez-Juste J (2015) Nanocrystal engineering of noble metals and metal chalcogenides: controlling the morphology, composition and crystallinity. CrystEngComm 17:3727–3762
6. Peddis D, Muscas G, Mathieu R, Kumar PA, Varvaro G, Singh G, Orue I, Gil-Carton D, Marcano L, Muela A, Fdez-Gubieda ML (2016) Studying nanoparticles' 3D shape by aspect maps: determination of the morphology of bacterial magnetic nanoparticles. Faraday Discuss 191:177–188
7. Versaci D, Costanzo A, Ronchetti SM, Onida B, Amici J, Francia C, Bodoardo S (2021) Ultrasmall SnO2 directly grown on commercial C45 carbon as lithium-ion battery anodes for long cycling performance. Electrochim Acta 367:137489
8. Balati A, Tek S, Nash K, Shipley H (2019) Nanoarchitecture of TiO2 microspheres with expanded lattice interlayers and its heterojunction to the laser modified black TiO2 using pulsed laser ablation in liquid with improved photocatalytic performance under visible light irradiation. J Colloid Interface Sci 541:234–248
9. Abouelela MM, Kawamura G, Matsuda A (2021) A review on plasmonic nanoparticle-semiconductor photocatalysts for water splitting. J Clean Prod 294:126200
10. Boken J, Khurana P, Thatai S, Kumar D, Prasad S (2017) Plasmonic nanoparticles and their analytical applications: a review. Appl Spectrosc Rev 52:774–820
11. Hu J, Ortgies DH, Rodríguez EM, Rivero F, Torres RA, Alfonso F, Fernández N, Carreño-Tarragona G, Monge L, Sanz-Rodriguez F, Iglesias MDC, Granado M, García-Villalon AL, Solé JG, Jaque D (2018) Optical nanoparticles for cardiovascular imaging. Adv Opt Mater 6:1800626
12. Alonso J, Barandiarán JM, Fernández Barquín L, García-Arribas A (2018) Magnetic nanoparticles, synthesis, properties, and applications. In: Magnetic Nanostructured Materials pp 1–40
13. Ng SM, Koneswaran M, Narayanaswamy R (2016) A review on fluorescent inorganic nanoparticles for optical sensing applications. RSC Adv 6:21624–21661
14. Kang H, Hu S, Cho MH, Hong SH, Choi Y, Choi HS (2018) Theranostic nanosystems for targeted cancer therapy. Nano Today 23:59–72
15. Xu X, Ray R, Gu Y, Ploehn HJ, Gearheart L, Raker K, Scrivens WA (2004) Electrophoretic analysis and purification of fluorescent single-walled carbon nanotube fragments. J Am Chem Soc 126:12736–12737
16. Goryacheva IY, Sapelkin AV, Sukhorukov GB (2017) Carbon nanodots: mechanisms of photoluminescence and principles of application. TrAC Trends Anal Chem 90:27–37
17. Barman MK, Patra A (2018) Current status and prospects on chemical structure driven photoluminescence behaviour of carbon dots. J Photochem Photobiol C Photochem Rev 37:1–22

18. Xiong Y, Schneider J, Ushakova EV, Rogach AL (2018) Influence of molecular fluorophores on the research field of chemically synthesized carbon dots. Nano Today 23:124–139
19. Liu Q, Ma C, Liu XP, Wei YP, Mao CJ, Zhu JJ (2017) A novel electrochemiluminescence biosensor for the detection of microRNAs based on a DNA functionalized nitrogen doped carbon quantum dots as signal enhancers. Biosens Bioelectron 92:273–279
20. Nguyen V, Si J, Yan L, Hou X (2016) Direct demonstration of photoluminescence originated from surface functional groups in carbon nanodots. Carbon 108:268–273
21. Li X, Zhang S, Kulinich SA, Liu Y, Zeng H (2014) Engineering surface states of carbon dots to achieve controllable luminescence for solid-luminescent composites and sensitive Be2+ detection. Sci Rep 4:4976
22. Farshbaf M, Davaran S, Rahimi F, Annabi N, Salehi R, Akbarzadeh A (2018) Carbon quantum dots: recent progresses on synthesis, surface modification and applications. Artificial cells, nanomedicine, and biotechnology 46:1331–1348
23. Huang YF, Zhou X, Zhou R, Zhang H, Kang KB, Zhao M, Peng Y, Wang Q, Zhang HL, Qiu WY (2014) One-pot synthesis of highly luminescent carbon quantum dots and their nontoxic ingestion by zebrafish for in vivo imaging. Chemistry 20:5640–5648
24. Kwon W, Do S, Rhee S-W (2012) Formation of highly luminescent nearly monodisperse carbon quantum dots via emulsion-templated carbonization of carbohydrates. RSC Adv 2:11223
25. Schwenke AM, Hoeppener S, Schubert US (2015) Synthesis and modification of carbon nanomaterials utilizing microwave heating. Adv Mater 27:4113–4141
26. Reyes D, Camacho M, Mayorga M, Weathers D, Salamo G, Wang Z, Neogi A (2016) Laser Ablated Carbon Nanodots for Light Emission. Nanoscale Res Lett 11:424
27. Kurdyukov DA, Eurov DA, Rabchinskii MK, Shvidchenko AV, Baidakova MV, Kirilenko DA, Koniakhin SV, Shnitov VV, Sokolov VV, Brunkov PN, Dideikin AT, Sgibnev YM, Mironov LY, Smirnov DA, Vul AY, Golubev VG (2018) Controllable spherical aggregation of monodisperse carbon nanodots. Nanoscale 10:13223–13235
28. Chandra S, Patra P, Pathan SH, Roy S, Mitra S, Layek A, Bhar R, Pramanik P, Goswami A (2013) Luminescent S-doped carbon dots: an emergent architecture for multimodal applications. J Mater Chem B 1:2375
29. Ge J, Jia Q, Liu W, Guo L, Liu Q, Lan M, Zhang H, Meng X, Wang P (2015) Red-emissive carbon dots for fluorescent, photoacoustic, and thermal theranostics in living mice. Adv Mater 27:4169–4177
30. Jiang K, Sun S, Zhang L, Lu Y, Wu A, Cai C, Lin H (2015) Red, green, and blue luminescence by carbon dots: full-color emission tuning and multicolor cellular imaging. Angew Chem Int Ed Engl 54:5360–5363
31. Liu Z, Zou H, Wang N, Yang T, Peng Z, Wang J, Li N, Huang C (2018) Photoluminescence of carbon quantum dots: coarsely adjusted by quantum confinement effects and finely by surface trap states. Sci China Chem 61:490–496
32. Zhang S, Zhang L, Huang L, Zheng G, Zhang P, Jin Y, Jiao Z, Sun X (2019) Study on the fluorescence properties of carbon dots prepared via combustion process. J Lumin 206:608–612
33. Loo AH, Sofer Z, Bousa D, Ulbrich P, Bonanni A, Pumera M (2016) Carboxylic carbon quantum dots as a fluorescent sensing platform for DNA detection. ACS Appl Mater Interfaces 8:1951–1957
34. Xu H, Yang X, Li G, Zhao C, Liao X (2015) Green synthesis of fluorescent carbon dots for selective detection of tartrazine in food samples. J Agric Food Chem 63:6707–6714
35. Park SY, Lee HU, Park ES, Lee SC, Lee JW, Jeong SW, Kim CH, Lee YC, Huh YS, Lee J (2014) Photoluminescent green carbon nanodots from food-waste-derived sources: large-scale synthesis, properties, and biomedical applications. ACS Appl Mater Interfaces 6:3365–3370
36. Chandra S, Mahto TK, Chowdhuri AR, Das B, Sahu SK (2017) One step synthesis of functionalized carbon dots for the ultrasensitive detection of Escherichia coli and iron (III). Sens Actuators B Chem 245:835–844
37. Jin H, Gui R, Wang Y, Sun J (2017) Carrot-derived carbon dots modified with polyethyleneimine and nile blue for ratiometric two-photon fluorescence turn-on sensing of sulfide anion in biological fluids. Talanta 169:141–148
38. Prasannan A, Imae T (2013) One-pot synthesis of fluorescent carbon dots from orange waste peels. Ind Eng Chem Res 52:15673–15678
39. Siddique AB, Pramanick AK, Chatterjee S, Ray M (2018) Amorphous carbon dots and their remarkable ability to detect 2,4,6-trinitrophenol. Sci Rep 8:9770
40. Arumugam N, Kim J (2018) Synthesis of carbon quantum dots from Broccoli and their ability to detect silver ions. Mater Lett 219:37–40
41. Zhu S, Meng Q, Wang L, Zhang J, Song Y, Jin H, Zhang K, Sun H, Wang H, Yang B (2013) Highly photoluminescent carbon dots for multicolor patterning, sensors, and bioimaging. Angew Chem Int Ed Engl 52:3953–3957
42. Gao P, Xie Z, Zheng M (2021) Small nanoparticles bring big prospect: the synthesis, modification, photoluminescence and sensing applications of carbon dots. Chin Chem Lett. https://doi.org/10.1016/j.cclet.2021.09.085
43. Su W, Wu H, Xu H, Zhang Y, Li Y, Li X, Fan L (2020) Carbon dots: a booming material for biomedical applications. Mater Chem Front 4:821–836
44. Azam N, Ali MN, Khan TJ (2021) Carbon quantum dots for biomedical applications: review and analysis. Front Mater 8:272
45. Chung YJ, Kim J, Park CB (2020) Photonic carbon dots as an emerging nanoagent for biomedical and healthcare applications. ACS Nano 14:6470–6497
46. Ghosal K, Ghosh A (2019) Carbon dots: the next generation platform for biomedical applications. Mater Sci Eng C, Mater Biol Appl 96:887–903
47. Kwon W, Do S, Kim JH, Seok Jeong M, Rhee SW (2015) Control of photoluminescence of carbon nanodots via surface functionalization using para-substituted anilines. Sci Rep 5:12604
48. Mao QX, E S, Xia JM, Song RS, Shu Y, Chen XW, Wang JH (2016) Hydrophobic carbon nanodots with rapid cell penetrability and tunable photoluminescence behavior for in vitro and in vivo imaging. Langmuir 32:12221–12229
49. Luo PG, Yang F, Yang S-T, Sonkar SK, Yang L, Broglie JJ, Liu Y, Sun Y-P (2014) Carbon-based quantum dots for fluorescence imaging of cells and tissues. RSC Adv 4:10791
50. Yang Y, Liu N, Qiao S, Liu R, Huang H, Liu Y (2015) Silver modified carbon quantum dots for solvent-free selective oxidation of cyclohexane. New J Chem 39:2815–2821
51. Yin B, Deng J, Peng X, Long Q, Zhao J, Lu Q, Chen Q, Li H, Tang H, Zhang Y, Yao S (2013) Green synthesis of carbon dots with down- and up-conversion fluorescent properties for sensitive detection of hypochlorite with a dual-readout assay. Analyst 138:6551–6557
52. Jia Q, Zhao Z, Liang K, Nan F, Li Y, Wang J, Ge J, Wang P (2020) Recent advances and prospects of carbon dots in cancer nanotheranostics. Mater Chem Front 4:449–471
53. Ray P, Moitra P, Pan D (2021) Emerging theranostic applications of carbon dots and its variants. View 3:20200089
54. Kong B, Yang T, Cheng F, Qian Y, Li C, Zhan L, Li Y, Zou H, Huang C (2022) Carbon dots as nanocatalytic medicine for anti-inflammation therapy. J Colloid Interface Sci 611:545–553
55. Yang X, Wang Y, Shen X, Su C, Yang J, Piao M, Jia F, Gao G, Zhang L, Lin Q (2017) One-step synthesis of photoluminescent carbon dots with excitation-independent emission for selective bioimaging and gene delivery. J Colloid Interface Sci 492:1–7
56. Mohammadi S, Salimi A, Hoseinkhani Z, Ghasemi F, Mansouri K (2022) Carbon dots hybrid for dual fluorescent detection of microRNA-21 integrated bioimaging of MCF-7 using a microfluidic platform. J Nanobiotechnology 20:73
57. Mohammadi R, Naderi-Manesh H, Farzin L, Vaezi Z, Ayarri N, Samandari L, Shamsipur M (2022) Fluorescence sensing and imaging with carbon-based quantum dots for early diagnosis of cancer: a review. J Pharm Biomed Anal 212:114628
58. Naik GG, Alam MB, Pandey V, Dubey PK, Parmar AS, Sahu AN (2020) Pink fluorescent carbon dots derived from the phytomedicine for breast cancer cell imaging. ChemistrySelect 5:6954–6960
59. Shi Y, Xu H, Yuan T, Meng T, Wu H, Chang J, Wang H, Song X, Li Y, Li X, Zhang Y, Xie W, Fan L (2021) Carbon dots: an innovative luminescent nanomaterial. Aggregate. https://doi.org/10.1002/agt2.108,e108
60. Yang X, Li X, Wang B, Ai L, Li G, Yang B, Lu S (2022) Advances, opportunities, and challenge for full-color emissive carbon dots. Chin Chem Lett 33:613–625
61. Hallaji Z, Bagheri Z, Kalji S-O, Ermis E, Ranjbar B (2021) Recent advances in the rational synthesis of red-emissive carbon dots for nanomedicine applications: a review. FlatChem 29:100271

62. Ding H, Zhou X-X, Wei J-S, Li X-B, Qin B-T, Chen X-B, Xiong H-M (2020) Carbon dots with red/near-infrared emissions and their intrinsic merits for biomedical applications. Carbon 167:322–344
63. Boruah JS, Sankaranarayanan K, Chowdhury D (2022) Insight into carbon quantum dot–vesicles interactions: role of functional groups. RSC Adv 12:4382–4394
64. Wareing TC, Gentile P, Phan AN (2021) Biomass-based carbon dots: current development and future perspectives. ACS Nano 15:15471–15501
65. Zhu Z, Cheng R, Ling L, Li Q, Chen S (2020) Rapid and large-scale production of multi-fluorescence carbon dots by a magnetic hyperthermia method. Angew Chem Int Ed Engl 59:3099–3105
66. Shaik SA, Sengupta S, Varma RS, Gawande MB, Goswami A (2020) Syntheses of N-doped carbon quantum dots (NCQDs) from bioderived precursors: a timely update. ACS Sustain Chem Eng 9:3–49
67. Zhou Y, Mintz KJ, Sharma SK, Leblanc RM (2019) Carbon dots: diverse preparation, application, and perspective in surface chemistry. Langmuir 35:9115–9132
68. Arcudi F, Dordevic L, Prato M (2019) Design, synthesis, and functionalization strategies of tailored carbon nanodots. Acc Chem Res 52:2070–2079
69. Alaghmandfard A, Sedighi O, Rezaei NT, Abedini AA, Khachatourian AM, Toprak MS, Seifalian A (2021) Recent advances in the modification of carbon-based quantum dots for biomedical applications. Mater Sci Eng C Mater Biol Appl 120:111756. https://doi.org/10.1016/j.msec.2020.111756
70. Anwar S, Ding H, Xu M, Hu X, Li Z, Wang J, Liu L, Jiang L, Wang D, Dong C, Yan M, Wang Q, Bi H (2019) Recent advances in synthesis, optical properties, and biomedical applications of carbon dots. ACS Appl Bio Mater 2:2317–2338
71. Li S, Li L, Tu H, Zhang H, Silvester DS, Banks CE, Zou G, Hou H, Ji X (2021) The development of carbon dots: from the perspective of materials chemistry. Mater Today 51:188–207
72. Godavarthi S, Mohan Kumar K, Vazquez Velez E, Hernandez-Eligio A, Mahendhiran M, Hernandez-Como N, Aleman M, Martinez Gomez L (2017) Nitrogen doped carbon dots derived from Sargassum fluitans as fluorophore for DNA detection. J Photochem Photobiol B 172:36–41
73. Khan S, Verma NC, Chethana, Nandi CK (2018) Carbon dots for single-molecule imaging of the nucleolus. ACS Appl Nano Mater 1:483–487
74. Shangguan J, He D, He X, Wang K, Xu F, Liu J, Tang J, Yang X, Huang J (2016) Label-Free carbon-dots-based ratiometric fluorescence pH nanoprobes for intracellular pH sensing. Anal Chem 88:7837–7843
75. Motaghi H, Mehrgardi MA, Bouvet P (2017) Carbon dots-AS1411 aptamer nanoconjugate for ultrasensitive spectrofluorometric detection of cancer cells. Sci Rep 7:10513
76. Zheng M, Li Y, Liu S, Wang W, Xie Z, Jing X (2016) One-pot to synthesize multifunctional carbon dots for near infrared fluorescence imaging and photothermal cancer therapy. ACS Appl Mater Interfaces 8:23533–23541
77. Wu L, Li X, Ling Y, Huang C, Jia N (2017) Morpholine derivative-functionalized carbon dots-based fluorescent probe for highly selective lysosomal imaging in living cells. ACS Appl Mater Interfaces 9:28222–28232
78. Wang HJ, He X, Luo TY, Zhang J, Liu YH, Yu XQ (2017) Amphiphilic carbon dots as versatile vectors for nucleic acid and drug delivery. Nanoscale 9:5935–5947
79. Das RK, Mohapatra S (2017) Highly luminescent, heteroatom-doped carbon quantum dots for ultrasensitive sensing of glucosamine and targeted imaging of liver cancer cells. J Mater Chem B 5:2190–2197
80. Brinker C, Scherer G (1990) Sol-gel science the physics and chemistry of sol-gel processing. Academic Press, Cambrdige
81. Stöber W, Fink A, Bohn E (1968) Controlled growth of monodisperse silica spheres in the micron size range. J Colloid Interface Sci 26:62–69
82. Jafarzadeh M, Rahman IA, Sipaut CS (2009) Synthesis of silica nanoparticles by modified sol–gel process: the effect of mixing modes of the reactants and drying techniques. J Sol-Gel Sci Technol 50:328–336
83. Tapec R, Zhao XJ, Tan W (2002) Development of organic dye-doped silica nanoparticles for bioanalysis and biosensors. J Nanosci Nanotechnol 2:405–409
84. Rahman IA, Vejayakumaran P, Sipaut CS, Ismail J, Bakar MA, Adnan R, Chee CK (2007) An optimized sol–gel synthesis of stable primary equivalent silica particles. Colloids Surf A Physicochem Eng Asp 294:102–110
85. Hun X, Bai L (2009) Synthesis of folate conjugated fluorescent nanoparticle probe and its application in cervical cancer cell imaging. Anal Lett 42:2280–2292
86. Liu S, Zhang HL, Liu TC, Liu B, Cao YC, Huang ZL, Zhao YD, Luo QM (2007) Optimization of the methods for introduction of amine groups onto the silica nanoparticle surface. J Biomed Mater Res, Part A 80:752–757
87. Samuel J, Raccurt O, Poncelet O, Auger A, Ling W-L, Cherns P, Grunwald D, Tillement O (2009) Surface characterizations of fluorescent-functionalized silica nanoparticles: from the macroscale to the nanoscale. J Nanoparticle Res 12:2255–2265
88. Thomassen LC, Aerts A, Rabolli V, Lison D, Gonzalez L, Kirsch-Volders M, Napierska D, Hoet PH, Kirschhock CE, Martens JA (2010) Synthesis and characterization of stable monodisperse silica nanoparticle sols for in vitro cytotoxicity testing. Langmuir 26:328–335
89. Lu H-T (2013) Synthesis and characterization of amino-functionalized silica nanoparticles. Colloid J 75:311–318
90. Liberman A, Mendez N, Trogler WC, Kummel AC (2014) Synthesis and surface functionalization of silica nanoparticles for nanomedicine. Surf Sci Rep 69:132–158
91. Greasley SL, Page SJ, Sirovica S, Chen S, Martin RA, Riveiro A, Hanna JV, Porter AE, Jones JR (2016) Controlling particle size in the Stober process and incorporation of calcium. J Colloid Interface Sci 469:213–223
92. Koźlecki T, Polowczyk I, Bastrzyk A, Sawiński W (2016) Improved synthesis of nanosized silica in water-in-oil microemulsions. J Nanoparticles 2016:8203260
93. Liu Z, Chen X, Zhang X, Gooding JJ, Zhou Y (2016) Carbon-quantum-dots-loaded mesoporous silica nanocarriers with pH-switchable zwitterionic surface and enzyme-responsive pore-cap for targeted imaging and drug delivery to tumor. Adv Healthc Mater 5:1401–1407
94. Ha SW, Camalier CE, Beck GR Jr, Lee JK (2009) New method to prepare very stable and biocompatible fluorescent silica nanoparticles. Chem Commun (Camb). https://doi.org/10.1039/b902195g,2881-2883
95. Hun X, Zhang Z (2007) Preparation of a novel fluorescence nanosensor based on calcein-doped silica nanoparticles, and its application to the determination of calcium in blood serum. Microchim Acta 159:255–261
96. Keasberry NA, Yapp CW, Idris A (2017) Mesoporous silica nanoparticles as a carrier platform for intracellular delivery of nucleic acids. Biochem Biokhimiia 82:655–662
97. Montalti M, Prodi L, Rampazzo E, Zaccheroni N (2014) Dye-doped silica nanoparticles as luminescent organized systems for nanomedicine. Chem Soc Rev 43:4243–4268
98. Rahmani S, Durand J-O, Charnay C, Lichon L, Férid M, Garcia M, Gary-Bobo M (2017) Synthesis of mesoporous silica nanoparticles and nanorods: application to doxorubicin delivery. Solid State Sci 68:25–31
99. Hernandez-Leon SG, Sarabia-Sainz JA, Montfort GR, Guzman-Partida AM, Robles-Burgueno MDR, Vazquez-Moreno L (2017) Novel synthesis of core-shell silica nanoparticles for the capture of low molecular weight proteins and peptides. Molecules 22:1712
100. Nallathamby PD, Hopf J, Irimata LE, McGinnity TL, Roeder RK (2016) Preparation of fluorescent Au–SiO2 core–shell nanoparticles and nanorods with tunable silica shell thickness and surface modification for immunotargeting. J Mater Chem B 4:5418–5428
101. Owens GJ, Singh RK, Foroutan F, Alqaysi M, Han C-M, Mahapatra C, Kim H-W, Knowles JC (2016) Sol–gel based materials for biomedical applications. Prog Mater Sci 77:1–79
102. Vera ML, Canneva A, Huck-Iriart C, Requejo FG, Gonzalez MC, Dell'Arciprete ML, Calvo A (2017) Fluorescent silica nanoparticles with chemically reactive surface: controlling spatial distribution in one-step synthesis. J Colloid Interface Sci 496:456–464
103. Tavernaro I, Cavelius C, Peuschel H, Kraegeloh A (2017) Bright fluorescent silica-nanoparticle probes for high-resolution STED and confocal microscopy. Beilstein J Nanotechnol 8:1283–1296
104. He X, Wang K, Li D, Tan W, He C, Huang S, Liu B, Lin X, Chen X (2007) A novel DNA-enrichment technology based on amino-modified functionalized silica nanoparticles. J Dispers Sci Technol 24:633–640

105. Burns A, Sengupta P, Zedayko T, Baird B, Wiesner U (2006) Core/Shell fluorescent silica nanoparticles for chemical sensing: towards single-particle laboratories. Small 2:723–726
106. Aruna K Munawar TM (2013) Surface modification of silicananoparticles for immobilize probe DNA to identify aspergillus flavus. In: International conference on advanced nanomaterials & emerging engineering technologies. IEEE; Chennai pp 148–149
107. Wang X, Song P, Peng L, Tong A, Xiang Y (2016) Aggregation-induced emission luminogen-embedded silica nanoparticles containing DNA aptamers for targeted cell imaging. ACS Appl Mater Interfaces 8:609–616
108. Yun H, Bang H, Min J, Chung C, Chang JK, Han DC (2010) Simultaneous counting of two subsets of leukocytes using fluorescent silica nanoparticles in a sheathless microchip flow cytometer. Lab Chip 10:3243–3254
109. Jiang WJ, Wu CL, Zhang RR (2012) General assembly of organic molecules in core-shell mesoporous silica nanoparticles. Mater Lett 77:100–102
110. Jiao Z, Li Z, Zhang H, Pan D, Xu P (2011) Self-assembly of novel core/shell structured blue fluorescent silica nanoparticles. J Control Relase 152:e262-263
111. Chen A, Mu H, Zuo C, Chen Y (2019) Fabrication, characterization, and CMP performance of dendritic mesoporous-silica composite particles with tunable pore sizes. J Alloys Compd 770:335–344
112. Kresge CT, Leonowicz ME, Roth WJ, Vartuli JC, Beck JS (1992) Ordered mesoporous molecular sieves synthesized by a liquid-crystal template mechanism. Nat Lett 359:710–712
113. Zhao D (1998) Triblock copolymer syntheses of mesoporous silica with periodic 50 to 300 angstrom pores. Science 279:548–552
114. Mehmood A, Ghafar H, Yaqoob S, Gohar UF, Ahmad B (2017) Mesoporous silica nanoparticles: a review. J Dev Drugs 6:174
115. Rahikkala A, Pereira SAP, Figueiredo P, Passos MLC, Araújo ARTS, Saraiva MLMFS, Santos HA (2018) Mesoporous silica nanoparticles for targeted and stimuli-responsive delivery of chemotherapeutics: a review. Adv Biosyst 2:1800020
116. Jafari S, Derakhshankhah H, Alaei L, Fattahi A, Varnamkhasti BS, Saboury AA (2019) Mesoporous silica nanoparticles for herapeutic/diagnostic applications. Biomed Pharmacother 109:1100–1111
117. Li QL, Wang D, Cui Y, Fan Z, Ren L, Li D, Yu J (2018) AIEgen-functionalized mesoporous silica gated by cyclodextrin-Modified CuS for cell imaging and chemo-photothermal cancer therapy. ACS Appl Mater Interfaces 10:12155–12163
118. Hurley MT, Wang Z, Mahle A, Rabin D, Liu Q, English DS, Zachariah MR, Stein D, DeShong P (2013) Synthesis, characterization, and application of antibody functionalized fluorescent silica nanoparticles. Adv Funct Mater 23:3335–3343
119. Yang KN, Zhang CQ, Wang W, Wang PC, Zhou JP, Liang XJ (2014) pH-responsive mesoporous silica nanoparticles employed in controlled drug delivery systems for cancer treatment. Cancer Biol Med 11:34–43
120. Vallet-Regi M, Balas F, Arcos D (2007) Mesoporous materials for drug delivery. Angew Chem Int Ed Engl 46:7548–7558
121. Regi-Vallet M, Rámila A, Del Real RP, Pariente-Pérez J (2001) A new property of MCM-41: drug delivery system. Chem Mater 13:308–311
122. Wu X, Wu M, Zhao JX (2014) Recent development of silica nanoparticles as delivery vectors for cancer imaging and therapy. Nanomed Nanotechnol Biol Med 10:297–312
123. Lin AL, Li SZ, Xu CH, Li XS, Zheng BY, Gu JJ, Ke MR, Huang JD (2018) A pH-responsive stellate mesoporous silica based nanophotosensitizer for in vivo cancer diagnosis and targeted photodynamic therapy. Biomaterials science 7:211–219
124. Cha BG, Kim J (2019) Functional mesoporous silica nanoparticles for bio-imaging applications. Wiley Interdiscip Rev Nanomed Nanobiotechnol 11:e1515
125. Singh RK, Patel KD, Leong KW, Kim HW (2017) Progress in nanotheranostics based on mesoporous silica nanomaterial platforms. ACS Appl Mater Interfaces 9:10309–10337
126. Bagwe RP, Hilliard LR, Tan W (2006) Surface modification of silica nanoparticles to reduce aggregation and nonspecific binding. Langmuir ACS J Surf Colloids 22:4357–4362
127. Christina AB, Chi G, Likens OQ, Brown SM (2017) A convenient, bio-inspired approach to the synthesis of multi-functional, stable fluorescent silica nanoparticles using poly (ethylene-imine). Nanoscale 2017:6509–6520
128. Kotsuchibashi Y, Ebara M, Aoyagi T, Narain R (2012) Fabrication of doubly responsive polymer functionalized silica nanoparticles via a simple thiol–ene click chemistry. Polym Chem 3:2545
129. Saroj S, Rajput SJ (2018) Composite smart mesoporous silica nanoparticles as promising therapeutic and diagnostic candidates: recent trends and applications. J Drug Deliv Sci Technol 44:349–365
130. Chen H, Wang GD, Sun X, Todd T, Zhang F, Xie J, Shen B (2016) Mesoporous silica as nanoreactors to prepare Gd-encapsulated carbon dots of controllable sizes and magnetic properties. Adv Funct Mater 26:3973–3982
131. Cabañas MV, Lozano D, Torres-Pardo A, Sobrino C, González-Calbet J, Arcos D, Vallet-Regí M (2018) Features of aminopropyl modified mesoporous silica nanoparticles. Implications on the active targeting capability. Mater Chem Phys 220:260–269
132. Sahu S, Sinha N, Bhutia SK, Majhi M, Mohapatra S (2014) Luminescent magnetic hollow mesoporous silica nanotheranostics for camptothecin delivery and multimodal imaging. J Mater Chem B 2:3799–3808
133. Tao C, Zhu Y (2014) Magnetic mesoporous silica nanoparticles for potential delivery of chemotherapeutic drugs and hyperthermia. Dalton Trans 43:15482–15490
134. Kim D, Kim J, Lee K-W, Lee TS (2019) Removal of sodium dodecylbenzenesulfonate using surface-functionalized mesoporous silica nanoparticles. Microporous Mesoporous Mater 275:270–277
135. Clemente A, Moreno N, Lobera MP, Balas F, Santamaria J (2018) Versatile hollow fluorescent metal-silica nanohybrids through a modified microemulsion synthesis route. J Colloid Interface Sci 513:497–504
136. Wang Y, Yin M, Lin X, Li L, Li Z, Ren X, Sun Y (2019) Tailored synthesis of polymer-brush-grafted mesoporous silicas with N-halamine and quaternary ammonium groups for antimicrobial applications. J Colloid Interface Sci 533:604–611
137. Du X, Qiao SZ (2015) Dendritic silica particles with center-radial pore channels: promising platforms for catalysis and biomedical applications. Small 11:392–413
138. Polshettiwar V, Cha D, Zhang X, Basset JM (2010) High-surface-area silica nanospheres (KCC-1) with a fibrous morphology. Angew Chem Int Ed Engl 49:9652–9656
139. Yang J, Chen W, Shen D, Wei Y, Ran X, Teng W, Fan J, Zhang W-X, Zhao D (2014) Controllable fabrication of dendritic mesoporous silica–carbon nanospheres for anthracene removal. J Mater Chem A 2:11045
140. Yang J, Shen D, Wei Y, Li W, Zhang F, Kong B, Zhang S, Teng W, Fan J, Zhang W, Dou S, Zhao D (2015) Monodisperse core-shell structured magnetic mesoporous aluminosilicate nanospheres with large dendritic mesochannels. Nano Res 8:2503–2514
141. Shen D, Yang J, Li X, Zhou L, Zhang R, Li W, Chen L, Wang R, Zhang F, Zhao D (2014) Biphase stratification approach to three-dimensional dendritic biodegradable mesoporous silica nanospheres. Nano Lett 14:923–932
142. Du X, Li X, Huang H, He J, Zhang X (2015) Dendrimer-like hybrid particles with tunable hierarchical pores. Nanoscale 7:6173–6184
143. Yu C, Abbaraju LP, Yang Y, Yu M, Fu J, Xu C (2017) Core-shell-structured dendritic mesoporous silica nanoparticles for combined photodynamic therapy and antibody delivery. Chem Asian J 12:1465–1469
144. Yano K, Fukushima Y (2004) Synthesis of mono-dispersed mesoporous silica spheres with highly ordered hexagonal regularity using conventional alkyltrimethylammonium halide as a surfactant. J Mater Chem B 14:1579
145. Sun Z, Li H, Cui G, Tian Y, Yan S (2016) Multifunctional magnetic core–shell dendritic mesoporous silica nanospheres decorated with tiny Ag nanoparticles as a highly active heterogeneous catalyst. Appl Surf Sci 360:252–262
146. Xing Y, Du X, Li X, Huang H, Li J, Wen Y, Zhang X (2018) Tunable dendrimer-like porous silica nanospheres: effects of structures and stacking manners on surface wettability. J Alloys Compd 732:70–79
147. Yamada N (1998) Photoluminescence from Carbon/Silica Gel Nanocomposite. In: Yoshimura S, Chang RPH (eds) Supercarbon. Springer Berlin Heidelberg, Berlin, pp 211–225
148. Yoshimura S, Chang RPH (1998) Supercarbon synthesis, properties and applications. Springer, Cham

149. Guo Z, Zhu Z, Zhang X, Chen Y (2018) Facile synthesis of blue-emitting carbon dots@mesoporous silica composite spheres. Solid State Sci 76:100–104
150. Zou Y, Yan F, Zheng T, Shi D, Sun F, Yang N, Chen L (2015) Highly luminescent organosilane-functionalized carbon dots as a nanosensor for sensitive and selective detection of quercetin in aqueous solution. Talanta 135:145–148
151. Kang MS, Singh RK, Kim TH, Kim JH, Patel KD, Kim HW (2017) Optical imaging and anticancer chemotherapy through carbon dot created hollow mesoporous silica nanoparticles. Acta Biomater 55:466–480
152. Yang W, Zhang G, Ni J, Lin Z (2020) Metal-enhanced fluorometric formaldehyde assay based on the use of in-situ grown silver nanoparticles on silica-encapsulated carbon dots. Mikrochim Acta 187:137
153. Zhao S, Sun S, Jiang K, Wang Y, Liu Y, Wu S, Li Z, Shu Q, Lin H (2019) In situ synthesis of fluorescent mesoporous silica–carbon dot nanohybrids featuring folate receptor-overexpressing cancer cell targeting and drug delivery. Nano-Micro Lett 11:32
154. da Silva ACP, de Freitas CF, Cardinali CAEF, Braga TL, Caetano W, Ravanelli MIB, Hioka N, Tessaro AL (2022) Biotin-functionalized silica nanoparticles loaded with Erythrosine B asselective photodynamic treatment for Glioblastoma Multiforme. J Mol Liq 345:117898
155. von Baeckmann C, Kahlig H, Linden M, Kleitz F (2021) On the importance of the linking chemistry for the PEGylation of mesoporous silica nanoparticles. J Colloid Interface Sci 589:453–461
156. Gao F, Lei C, Liu Y, Song H, Kong Y, Wan J, Yu C (2021) Rational design of dendritic mesoporous silica nanoparticles' surface chemistry for quantum dot enrichment and an ultrasensitive lateral flow immunoassay. ACS Appl Mater Interfaces 13:21507–21515
157. Sreejith S, Kishor R, Abbas A, Thomas R, Yeo T, Ranjan VD, Vaidyanathan R, Seah YP, Xing B, Wang Z, Zeng L, Zheng Y, Lim CT (2019) Nanomechanical microfluidic mixing and rapid labeling of silica nanoparticles using allenamide-thiol covalent linkage for bioimaging. ACS Appl Mater Interfaces 11:4867–4875
158. Hasany M, Taebnia N, Yaghmaei S, Shahbazi MA, Mehrali M, Dolatshahi-Pirouz A, Arpanaei A (2019) Silica nanoparticle surface chemistry: an important trait affecting cellular biocompatibility in two and three dimensional culture systems. Colloids Surf B Biointerfaces 182:110353
159. Zou C, Foda MF, Tan X, Shao K, Wu L, Lu Z, Bahlol HS, Han H (2016) Carbon-dot and quantum-dot-coated dual-emission core-satellite silica nanoparticles for ratiometric intracellular Cu(2+) imaging. Anal Chem 88:7395–7403
160. Innocenzi P, Malfatti L, Carboni D (2015) Graphene and carbon nanodots in mesoporous materials: an interactive platform for functional applications. Nanoscale 7:12759–12772
161. Malfatti L, Innocenzi P (2018) Sol-gel chemistry for carbon dots. Chem Rec 18:1192–1202
162. Prasad R, Aiyer S, Chauhan DS, Srivastava R, Selvaraj K (2016) Bioresponsive carbon nano-gated multifunctional mesoporous silica for cancer theranostics. Nanoscale 8:4537–4546
163. Augustine S, Singh J, Srivastava M, Sharma M, Das A, Malhotra BD (2017) Recent advances in carbon based nanosystems for cancer theranostics. Biomater Sci 5:901–952
164. Tang H, Wang M, Meng C, Tao W, Wang C, Yu H (2019) Research on design, fabrication, and properties of Fe2O3@SiO2/CDs/PEG@nSiO2 nanocomposites. Mater Lett 235:39–41
165. Zhang Q, Li X, Peng L, Zou X, Zhao Y (2021) Porous silica nanoparticles capped with polyethylenimine/green carbon dots for pH/redox responsive drug release. Inorg Chem Commun 123:108340
166. He L, Zhang H, Fan H, Jiang X, Zhao W, Xiang GQ (2018) Carbon-dot-based dual-emission silica nanoparticles as a ratiometric fluorescent probe for vanadium(V) detection in mineral water samples. Spectrochim Acta A Mol Biomol Spectrosc 189:51–56
167. Gao G, Jiang Y-W, Jia H-R, Yang J, Wu F-G (2018) On-off-on fluorescent nanosensor for Fe3+ detection and cancer/normal cell differentiation via silicon-doped carbon quantum dots. Carbon 134:232–243
168. Cui C, Lei J, Yang L, Shen B, Wang L, Zhang J (2018) Carbon-dot-encapsulated molecularly imprinted mesoporous organosilica for fluorescent sensing of rhodamine 6G. Res Chem Intermed 44:4633–4640
169. Yadav RK, Kumar A, Park N-J, Yadav D, Baeg J-O (2017) New carbon nanodots-silica hybrid photocatalyst for highly selective solar fuel production from CO2. ChemCatChem 9:3153–3159
170. Tian Y, Zhipeng R, Yang W (2017) Carbon dot-silica composite nanoparticle: an excitation-independent fluorescence material with tunable fluorescence. RSC Adv 7:43839–43844
171. Sciortino L, Messina F, Buscarino G, Agnello S, Cannas M, Gelardi FM (2017) Nitrogen-doped carbon dots embedded in a SiO2 monolith for solid-state fluorescent detection of Cu2+ ions. J Nanopart Res 19:228
172. Xiang G, Wang Y, Zhang H, Fan H, Fan L, He L, Jiang X, Zhao W (2018) Carbon dots based dual-emission silica nanoparticles as ratiometric fluorescent probe for nitrite determination in food samples. Food Chem 260:13–18
173. Amjadi M, Jalili RA (2018) molecularly imprinted dual-emission carbon dot-quantum dot mesoporous hybrid for ratiometric determination of anti-inflammatory drug celecoxib. Spectrochim Acta Part A Mol Biomol Spectrosc 191:345–351
174. BelBruno JJ (2018) Molecularly imprinted polymers. Chem Rev 20191:94–119
175. Chen L, Wang X, Lu W, Wu X, Li J (2016) Molecular imprinting: perspectives and applications. Chem Soc Rev 45:2137–2211
176. Hashemi-Moghaddam H, Mowla SJ, Nouraee N (2016) Separation of microRNA 21 as a cancer marker from glioblastoma cell line using molecularly imprinted polymer coated on silica nanoparticles. J Sep Sci 39:3564–3570
177. Demir B, Lemberger MM, Panagiotopoulou M, Medina Rangel PX, Timur S, Hirsch T, Tse Sum Bui B, Wegener J, Haupt K (2018) Tracking hyaluronan: molecularly imprinted polymer coated carbon dots for cancer cell targeting and imaging. ACS Appl Mater Interfaces 10:3305–3313
178. Shirani MP, Rezaei B, Ensafi AA (2019) A novel optical sensor based on carbon dots embedded molecularly imprinted silica for selective acetamiprid detection. Spectrochim Acta A Mol Biomol Spectrosc 210:36–43
179. Lv P, Xie D, Zhang Z (2018) Magnetic carbon dots based molecularly imprinted polymers for fluorescent detection of bovine hemoglobin. Talanta 188:145–151
180. Amjadi M, Jalili R (2017) Molecularly imprinted mesoporous silica embedded with carbon dots and semiconductor quantum dots as a ratiometric fluorescent sensor for diniconazole. Biosens Bioelectron 96:121–126
181. Sharma SN, Pillai ZS, Kamat VP (2003) Photoinduced charge transfer between CdSe quantum dots and p-phenylenediamine. J Phys Chem B 107:10088–10093
182. Zhang Y, Jing P, Zeng Q, Sun Y, Su Y, Wang YA, Kong X, Zhao J, Zhang H (2009) Photoluminescence quenching of CdSe core/shell quantum dots by hole transporting materials. J Phys Chem C 113:1886–1890
183. Shariati R, Rezaei B, Jamei HR, Ensafi AA (2019) Application of coated green source carbon dots with silica molecularly imprinted polymers as a fluorescence probe for selective and sensitive determination of phenobarbital. Talanta 194:143–149
184. Teymoorian T, Hashemi N, Mousazadeh MH, Entezarian Z (2021) N, S doped carbon quantum dots inside mesoporous silica for effective adsorption of methylene blue dye. SN Appl Sci 3:305
185. Dong Y, Ma J, Liu C, Bao Y (2020) Ordered mesoporous silica encapsulated carbon quantum dots and its application in Fe3+ detection. Ceram Int 46:11115–11123
186. Amiri A, Faridbod F, Zoughi S (2021) An optical nanosensor fabricated by carbon dots embedded in silica molecularly imprinted polymer for sensitive detection of ceftazidime antibiotic. J Photochem Photobiol A Chem 408:113111
187. Liu G, Chen Z, Jiang X, Feng D-Q, Zhao J, Fan D, Wang W (2016) In-situ hydrothermal synthesis of molecularly imprinted polymers coated carbon dots for fluorescent detection of bisphenol A. Sens Actuators B Chem 228:302–307
188. Yang J, Lin ZZ, Nur AZ, Lu Y, Wu MH, Zeng J, Chen XM, Huang ZY (2018) Detection of trace tetracycline in fish via synchronous fluorescence quenching with carbon quantum dots coated with molecularly imprinted silica. Spectrochim Acta Part A Mol Biomol Spectrosc 190:450–456
189. Wang R, Li G, Dong Y, Chi Y, Chen G (2013) Carbon quantum dot-functionalized aerogels for NO2 gas sensing. Anal Chem 85:8065–8069
190. Wang L, Zhang H, Zhou X, Liu Y, Lei B (2016) Preparation, characterization and oxygen sensing properties of luminescent carbon dots assembled mesoporous silica microspheres. J Colloid Interface Sci 478:256–262

191. Danielsson I, Lindman B (1981) The definition of microemulsion. Colloids Surf 3:391–392
192. Moulik SP, Animesh KR (2006) Physicochemistry and applications of micro-emulsions. J Surface Sci Technol 22:159–118
193. Flores ME, Martinez F, Olea AF, Shibue T, Sugimura N, Nishide H, Moreno-Villoslada I (2017) Water-induced phase transition in Cyclohexane/n-Hexanol/Triton X-100 mixtures at a molar composition of 1/16/74 studied by NMR. J Phys Chem B 121:876–882
194. McClements DJ (2012) Nanoemulsions versus microemulsions: terminology, differences, and similarities. Soft Matter 8:1719–1729
195. Stubenrauch C (2008) Microemulsions- background, new concepts, applications Wiley-Blackwell, New Jersey
196. Magno M, Angelescu DG, Stubenrauch C (2009) Phase diagrams of non-ionic microemulsions containing reducing agents and metal salts as bases for the synthesis of bimetallic nanoparticles. Colloids Surf A Physicochem Eng Asp 348:116–123
197. Ganguli AK, Ganguly A, Vaidya S (2010) Microemulsion-based synthesis of nanocrystalline materials. Chem Soc Rev 39:474–485
198. Pasquali RC, Taurozzi MP, Bregni C (2008) Some considerations about the hydrophilic-lipophilic balance system. Int J Pharm 356:44–51
199. Jaramillo N, Paucar C, García C (2014) Influence of the reaction time and the Triton x–100/Cyclohexane/Methanol/H2O ratio on the morphology and size of silica nanoparticles synthesized via sol–gel assisted by reverse micelle microemulsion. J Mater Sci 49:3400–3406
200. Wang J, Tsuzuki T, Sun L, Wang X (2010) Reverse microemulsion-mediated synthesis of SiO(2)-coated ZnO composite nanoparticles: multiple cores with tunable shell thickness. ACS Appl Mater Interfaces 2:957–960
201. Qui S, Dong J, Chen G (1999) Preparation of Cu nanoparticles from water-in-oil microemulsions. J Colloid Interface Sci 216:230–234
202. Biswas S, Hait SK, Bhattacharya SC, Moulik SP (2005) Synthesis of nanoparticles of CuI, CuCrO4, and CuS in Water/AOT/Cyclohexanone and Water/TX-100 + i-propanol/cyclohexanone reverse microemulsions. J Dispers Sci Technol 25:801–816
203. Li J, Yang X, Yang P, Gao F (2016) Hyaluronic acid–conjugated silica nanoparticles for breast cancer therapy. Inorg Nano-Met Chem 47:777–782
204. Giovannini G, Kunc F, Piras CC, Stranik O, Edwards AA, Hall AJ, Gubala V (2017) Stabilizing silica nanoparticles in hydrogels: impact on storage and polydispersity. RSC Adv 7:19924–19933
205. Chen Q, Shen X, Gao H (2007) Formation of nanoparticles in water-in-oil microemulsions controlled by the yield of hydrated electron: the controlled reduction of Cu2+. J Colloid Interface Sci 308:491–499
206. Richard B, Lemyre J-L, Ritcey AM (2017) Nanoparticle size control in microemulsion synthesis. Langmuir ACS J Surf Colloids 33:4748–4757
207. Tojo C, Blanco MC, Rivadulla F, López-Quintela MA (1997) Kinetics of the formation of particles in microemulsions. Langmuir ACS J Surf Colloids 13:1970–1977
208. Wang W, Fu X-A, Tang J-A, Jiang L (1993) Preparation of submicron spherical particles of silica by the water-in-oil microemulsion method. Colloids Surf A Physicochem Eng Asp 81:177–180
209. Hristov DR, Mahon E, Dawson AK (2015) Controlling aqueous silica nanoparticle synthesis in the 10–100 nm range. Chem Commun 51:17420–17423
210. Bagwe RP, Yang C, Hilliard LR, Tan W (2004) Optimization of dye-doped silica nanoparticles prepared using a reverse microemulsion method. Langmuir ACS J Surf Colloids 20:8336–8342
211. Arriagada FJ, Osseo-Assare K (1998) Synthesis of nanosize silica in a non-ionic water-in-oil microemulsion: effects of the water/surfactant molar ratio and ammonia concentration. J Colloid Interface Sci 211:210–220
212. Sun Y, Wang X, Wu J, Fu Y, Zhang J, Li H, Li W (2010) Effects of surfactant/water ratio and dye amount on the fluorescent silica nanoparticles. Colloid J 72:723–729
213. Abarkan I, Doussineau T, Smaïhi M (2006) Tailored macro/microstructural properties of colloidal silica nanoparticles via microemulsion preparation. Polyhedron 25:1763–1770
214. Gustafsson H, Isaksson S, Altskar A, Holmberg K (2016) Mesoporous silica nanoparticles with controllable morphology prepared from oil-in-water emulsions. J Colloid Interface Sci 467:253–260
215. Liu X, Zhang N, Bing T, Shangguan D (2014) Carbon dots based dual-emission silica nanoparticles as a ratiometric nanosensor for Cu(2+). Anal Chem 86:2289–2296
216. Dong Y, Wang R, Li G, Chen C, Chi Y, Chen G (2012) Polyamine-functionalized carbon quantum dots as fluorescent probes for selective and sensitive detection of copper ions. Anal Chem 84:6220–6224
217. Molaei MJ (2019) A review on nanostructured carbon quantum dots and their applications in biotechnology, sensors, and chemiluminescence. Talanta 196:456–478
218. Ji C, Zhou Y, Leblanc RM, Peng Z (2020) Recent developments of carbon dots in biosensing: a review. ACS sensors 5:2724–2741
219. Qiao Y, Liu C, Zheng X (2018) Enhancing the quantum yield and Cu2+ sensing sensitivity of carbon dots based on the nano-space confinement effect of silica matrix. Sens Actuators B Chem 259:211–218
220. Han X, Han Y, Huang H, Zhang H, Zhang X, Liu R, Liu Y, Kang Z (2013) Synthesis of carbon quantum dots/SiO2 porous nanocomposites and their catalytic ability for photo-enhanced hydrocarbon selective oxidation. Dalton Trans 42:10380–10383
221. Wei JM, Liu BT, Zhang X, Song CC (2018) One-pot synthesis of N, S co-doped photoluminescent carbon quantum dots for Hg2+ ion detection. New Carbon Mater 33:333–340
222. Mintz K, Waidely E, Zhou Y, Peng Z, Al-Youbi AO, Bashammakh AS, El-Shahawi MS, Leblanc RM (2018) Carbon dots and gold nanoparticles based immunoassay for detection of alpha-L-fucosidase. Anal Chim Acta 1041:114–121
223. Wu Y, Wei P, Pengpumkiat S, Schumacher EA, Remcho VT (2016) A novel ratiometric fluorescent immunoassay for human α-fetoprotein based on carbon nanodot-doped silica nanoparticles and FITC. Anal Methods 8:5398–5406
224. Lee JE, Lee N, Kim T, Kim J, Hyeon T (2011) Multifunctional mesoporous silica nanocomposite nanoparticles for theranostic applications. Acc Chem Res 44:893–902
225. Zhao Q, Wang S, Yang Y, Li X, Di D, Zhang C, Jiang T (2017) Hyaluronic acid and carbon dots-gated hollow mesoporous silica for redox and enzyme-triggered targeted drug delivery and bioimaging. Mater Sci Eng C Mater Biol Appl 78:475–484
226. Schladt TD, Schneider K, Schild H, Tremel W (2011) Synthesis and bio-functionalization of magnetic nanoparticles for medical diagnosis and treatment. Dalton Trans 40:6315–6343
227. Das S, Debnath N, Cui Y, Unrine J, Palli SR (2015) Chitosan, carbon quantum dot, and silica nanoparticle mediated dsRNA delivery for gene silencing in aedes aegypti: a comparative analysis. ACS Appl Mater Interfaces 7:19530–19535
228. Kim J, Park J, Kim H, Singha K, Kim WJ (2013) Transfection and intracellular trafficking properties of carbon dot-gold nanoparticle molecular assembly conjugated with PEI-pDNA. Biomaterials 34:7168–7180
229. Sood A, Arora V, Shah J, Kotnala RK, Jain TK (2017) Multifunctional gold coated iron oxide core-shell nanoparticles stabilized using thiolated sodium alginate for biomedical applications. Mater Sci Eng C Mater Biol Appl 80:274–281
230. Das RK, Pramanik A, Majhi M, Mohapatra S (2018) Magnetic mesoporous silica gated with doped carbon dot for site-specific drug delivery, fluorescence, and MR imaging. Langmuir ACS J Surf Colloids 34:5253–5262
231. Rashid M, Ahmad QZ, Tajuddin (2019) Trends in nanotechnology for practical applications. In: Mohapatra SS, Ranjan S, Dasgupta N, Mishra RK, Thomas S (eds) Applications of targeted nano drugs and delivery systems. Elsevier, Amsterdam
232. Wang Y, Shi W, Wang S, Li C, Qian M, Chen J, Huang R (2016) Facile incorporation of dispersed fluorescent carbon nanodots into mesoporous silica nanosphere for pH-triggered drug delivery and imaging. Carbon 108:146–153
233. Pathak C, Vaidya FU, Pandey SM (2019) Mechanism for development of nanobased drug delivery system. In: Mohapatra SS, Ranjan S, Dasgupta N, Mishra RK, Thomas S (eds) Applications of targeted nano drugs and delivery systems. Elsevier, Amsterdam
234. Cho K, Wang X, Nie S, Chen ZG, Shin DM (2008) Therapeutic nanoparticles for drug delivery in cancer. Clin Cancer Res Official J American Assoc Cancer Res 14:1310–1316
235. Wu D, Si M, Xue HY, Wong HL (2017) Nanomedicine applications in the treatment of breast cancer: current state of the art. Int J Nanomed 12:5879–5892

236. Manaia EB, Abucafy MP, Chiari-Andreo BG, Silva BL, Oshiro Junior JA, Chiavacci LA (2017) Physicochemical characterization of drug nanocarriers. Int J Nanomed 12:4991–5011
237. Mo R, Gu Z (2016) Tumor microenvironment and intracellular signal-activated nanomaterials for anticancer drug delivery. Mater Today 19:274–283
238. Truong NP, Whittaker MR, Mak CW, Davis TP (2015) The importance of nanoparticle shape in cancer drug delivery. Expert Opin Drug Deliv 12:129–142
239. Banerjee A, Qi J, Gogoi R, Wong J, Mitragotri S (2016) Role of nanoparticle size, shape and surface chemistry in oral drug delivery. Journal of controlled release : official journal of the Controlled Release Society 238:176–185
240. Zhao T, Chen L, Li Q, Li X (2018) Near-infrared light triggered drug release from mesoporous silica nanoparticles. J Mater Chem B 6:7112–7121
241. Jindal AB (2017) The effect of particle shape on cellular interaction and drug delivery applications of micro- and nanoparticles. Int J Pharm 532:450–465
242. Delic A, Mariussen E, Roede ED, Krivokapic A, Erbe A, Lindgren M, Benelmekki M, Einarsrud MA (2021) Fluorescent nanocomposites: hollow silica microspheres with embedded carbon dots. ChemPlusChem 86:176–183
243. Chen Y, Li X, Zhao Y, Zhang X, Sun L (2020) Preparation of triple-responsive porous silica carriers and carbon quantum dots for photodynamic-/chemotherapy and multicolor cell imaging. ChemNanoMat 6:648–656
244. Zhou B, Guo Z, Lin Z, Zhang L, Jiang B-P, Shen X-C (2019) Recent insights into near-infrared light-responsive carbon dots for bioimaging and cancer phototherapy. Inorg Chem Front 6:1116–1128
245. Sun S, Zhao S, Jiang K, Wang Y, Shu Q, Jin S, Li Z, Lin H (2020) A facile approach to carbon dots-mesoporous silica nanohybrids and their applications for multicolor and two-photon imaging guided chemo-/photothermal synergistic oncotherapy. ChemNanoMat 6:953–962
246. Chen Y, Zhao Y, Zou X, Sun L (2021) Porous silica nanocarriers with gold/carbon quantum dots for photo-chemotherapy and cellular imaging. J Drug Deliv Sci Technol 61:102141
247. Liu Y, Liu X, Xiao Y, Chen F, Xiao F (2017) A multifunctional nanoplatform based on mesoporous silica nanoparticles for imaging-guided chemo/photodynamic synergetic therapy. RSC Adv 7:31133–31141
248. Slowing II, Vivero-Escoto JL, Wu CW, Lin VS (2008) Mesoporous silica nanoparticles as controlled release drug delivery and gene transfection carriers. Adv Drug Deliv Rev 60:1278–1288
249. He Z, Liu K, Byrne HJ, Cullen PJ, Tian F, Curtin JF (2019) Combination strategies for targeted delivery of nanoparticles for cancer therapy. In: Mohapatra S, Ranjan S, Dasgupta D, Mishra R, Thomas S (eds) Applications of targeted nano drugs and delivery systems: nanoscience and nanotechnology in drug delivery. Elseveir, Amsterdam, pp 191–219
250. Zhao L, Ren X, Zhang J, Zhang W, Chen X, Meng X (2020) Dendritic silica with carbon dots and gold nanoclusters for dual nanozymes. New J Chem 44:1988–1992
251. Chavda VP (2019) Nanobased nano drug delivery: a comprehensive review. In: Mohapatra S, Ranjan S, Dasgupta N, Kumar R, Thomas S (eds) Applications of targeted nano drugs and delivery systems. Elsevier, Amsterdam, pp 69–92
252. Shirani MP, Rezaei B, Khayamian T, Dinari M, Shamili FH, Ramezani M, Alibolandi M (2018) Ingenious pH-sensitive etoposide loaded folic acid decorated mesoporous silica-carbon dot with carboxymethyl-betacyclodextrin gatekeeper for targeted drug delivery and imaging. Mater Sci Eng C Mater Biol Appl 92:892–901
253. Li X, Wang W, Li Q, Lin H, Xu Y, Zhuang L (2018) Design of Fe3O4@SiO2@mSiO2-organosilane carbon dots nanoparticles: synthesis and fluorescence red-shift properties with concentration dependence. Mater Des 151:89–101
254. Mohapatra S, Sahu S, Nayak S, Ghosh SK (2015) Design of Fe(3)O(4)@SiO(2)@carbon quantum dot based nanostructure for fluorescence sensing, magnetic separation, and live cell imaging of fluoride ion. Langmuir 31:8111–8120
255. Wang M, Fu Q, Zhang K, Wan Y, Wang L, Gao M, Xia Z, Gao D (2019) A magnetic and carbon dot based molecularly imprinted composite for fluorometric detection of 2,4,6-trinitrophenol. Mikrochim Acta 186:86
256. Liu X, Liu L, Hu X, Zhou S, Ankri R, Fixler D, Xie Z (2018) Multimodal bioimaging based on gold nanorod and carbon dot nanohybrids as a novel tool for atherosclerosis detection. Nano Res 11:1262–1273

Publisher's Note

Springer Nature remains neutral with regard to jurisdictional claims in published maps and institutional affiliations.

Submit your manuscript to a SpringerOpen journal and benefit from:

- ► Convenient online submission
- ► Rigorous peer review
- ► Open access: articles freely available online
- ► High visibility within the field
- ► Retaining the copyright to your article

Submit your next manuscript at ► springeropen.com